A computationally designed Rituximab/CD3 T cell engager targeting CD20+ cancers with multiple mechanisms of action

Wenyan Cai
Genor Biopharma Co. Ltd.
Jianbo Dong
Ab Studio Inc.
Sachith Gallolu Kankanamalage
Ab Studio Inc.
Allison Titong
Ab Studio Inc.
Jiadong Shi
Ab Studio Inc.
Zhejun Jia
Ab Studio Inc.
Bo Wang
Ab Studio Inc.
Cai Huang
Ab Therapeutics Inc.
Jing Zhang
Genor Biopharma Co. Ltd.
Jun Lin
Genor Biopharma Co. Ltd.
Steven Z. Kan
Genor Biopharma Co. Ltd.
Joe Zhou
Genor Biopharma Co. Ltd.
Yue Liu (yue.liu@antibodystudio.com)
Ab Studio Inc.

Research Article

Keywords: T cell engaging antibodies, safety, expanded mechanisms, heavy chain complementarity-determining regions, Rituximab arm

Posted Date: March 17th, 2021

DOI: https://doi.org/10.21203/rs.3.rs-292346/v1

Version of Record: A version of this preprint was published at Antibody Therapeutics on October 22nd, 2021. See the published version at https://doi.org/10.1093/abt/tbab024.

A computationally designed Rituximab/CD3 T cell engager targeting CD20+ cancers with multiple mechanisms of action

*Wenyan Cai[1,3], *Jianbo Dong[1], Sachith Gallolu Kankanamalage[1], Allison Titong[1], Jiadong Shi[1], Zhejun Jia[1], Bo Wang[1], Cai Huang [2] Jing Zhang[3], Jun Lin[3], Steven Z. Kan[3], Joe Zhou[3], and Yue Liu[1,2]

[1] Ab Studio Inc., 3541 Investment Blvd., Suite 3, Hayward, CA 94545

[2] Ab Therapeutics Inc., a JHBP company, 3541 Investment Blvd., Suite 2, Hayward, CA 94545

[3] Genor Biopharma Co. Ltd., a JHBP company, 1690 Zhangheng Road, Building 3, Pudong New District, Shanghai, P.R.C.

*These authors contributed equally to this work

To whom correspondence should be address:

Yue Liu, Ph.D.

Ab Studio Inc.,

3541 Investment Blvd.

Suite 3

Hayward, CA 94545

yue.liu@antibodystudio.com

ABSTRACT

Bispecific T cell engaging antibodies (TEAs) with one arm targeting a cancer antigen and another arm binding to CD3 have demonstrated impressive efficacy in multiple clinical studies. However, establishing a safety/efficacy balance remains challenging. For instance, some TEAs have severe safety issues. Additionally, not all patients or all cancer cells of one patient respond equally to TEAs. Here, we developed a next-generation bispecific TEA with better safety/efficacy balance and expanded mechanisms of action. Using the computer aided antibody design strategy, we replaced heavy chain complementarity-determining regions (HCDRs) in one Rituximab arm with HCDRs from a CD3 antibody and generated a novel CD20/CD3 bispecific antibody. After series of computer aided sequence optimization, the lead molecule, GB261, showed great safety/efficacy balance both in vitro and in animal studies. GB261 exhibited high affinity to CD20 and ultra-low affinity to CD3. It showed comparable T cell activation and reduced cytokine secretion compared to a benchmark antibody (BM). GB261-induced ADCC and CDC only killed CD20+ cells but not CD3+ cells. It exhibited better RRCL cell killing than the BM in a PBMC engrafted, therapeutic treatment mouse model and good safety in cynomolgus monkeys. Thus, GB261 is a promising novel TEA against CD20+ cancers.

INTRODUCTION

Immunotherapy that utilizes the body's immune system against tumors is a promising field of cancer research [1-3]. In recent years, exciting technologies and platforms have been developed for the intricate design and production of anticancer immune reagents such as antibodies and CAR-T cells [4-7]. Among these, bispecific T-cell-engaging antibodies (TEA) have attracted a lot of interest [8-11]. BiTE, the most well-known TEA, is a recombinant bispecific protein that has two linked scFvs from two different antibodies, one targeting a cell-surface molecule on T cells (for example, CD3ε) and another targeting antigens on the surface of malignant cells [10,12,13]. BiTEs bind to tumor antigens and T cells simultaneously, and mediate T-cell responses, thus killing tumor cells. While BiTEs have the advantages of relatively simple recombinant production and purification, and a molecular weight enabling tissue penetration, they also have disadvantages of short half-life (2.1hrs) and inconvenient drug administration (infusion pump needed) [14]. Recently, scientists from Genentech and Regeneron reported novel bispecific TEA with native human IgG format, which target CD20, a B cell marker, and the CD3 component of the T cell receptor, triggering redirected killing of B cells [15,16]. For example, it was shown that in cynomolgus monkeys, low doses of REGN1979 (CD20/CD3 bispecific antibody (BsAb)) caused prolonged depletion of B cells in peripheral blood with a serum half-life of approximately 14 days [15]. A phase I clinical trial study suggested that REGN1979 has acceptable safety profile as well as preliminary antitumor activity [17]. While most IgG-like bispecific TEAs show promising efficacy *in vitro* and *in vivo*, some of them have safety concerns to be addressed [18-20]. For instance, REGN1979 caused two deaths in clinical studies because it elicited cytokine release syndrome (CRS) [20]. Other than safety concerns, another limitation for almost all current IgG-like bispecific TEAs is lack of Fc effector functions: antibody-dependent cellular cytotoxicity (ADCC) and complement-dependent cytotoxicity (CDC), which are the major functions of Rituximab, a widely used anti CD20+ tumor monoclonal antibody[21,22]. This may limit the benefits of these BsAbs to

certain patients who respond to ADCC and/or CDC. To resolve these problems and develop the next generation of bispecific TEAs with better safety and more mechanisms of action for targeting cancer heterogeneity and diverse cancer drug resistance, we designed a novel CD20/CD3 BsAb, GB261, with ultra-low CD3 binding affinity, which allows efficient T cell activation only in the presence of CD20+ target cells but not in the presence of CD20- cells. Because this novel BsAb retains ADCC and CDC functions that targets CD20+ cancer cells only, but not CD3+ T cells *in vitro*, it has potential to trigger cancer cell killing faster and more efficiently in pathophysiological settings where the T/B cell ratios are extremely low. The reason for this effect is that even before encountering T cells, it could kill cancer cells via ADCC/CDC immediately after being injected. This initial cancer cell killing event may enhance the T cell/cancer cell ratio and the chance for BsAb to engage T cells. Once the BsAb binds to both cancer cells and T cells, it activates T cells and further induces T cells-mediated cancer cell killing. In addition, the enhanced ratio of natural killer (NK) cells and macrophages to cancer cells would further increase the ADCC/CDC/Antibody-dependent cellular phagocytosis (ADCP) functions, thereby further exacerbating the cancer cell killing. Because of this novel mechanism, GB261 can be a better therapeutic candidate compared to other CD20/CD3 BsAbs.

To design GB261, we employed the computer aided antibody design (CAAD) strategy. With this, we designed multiple common VLs and selected the VL of Rituximab as the lead common VL, replaced the heavy chain complementarity-determining region (HCDR) of one Rituximab arm with CD3 HCDRs, modified these parental VH sequences to differentiate their chemico-physical characteristics, reduced the immunogenicity of the BsAb, increased the stability of the BsAb via backmutations, humanized the VH regions, and introduced mutations in the Fc domain to enhance heterodimer formation. The CAAD was preferred over the traditional antibody discovery methods because CAAD significantly decreases the timeframe of antibody development. CAAD can be used to generate structural modifications easily and more successfully in the therapeutic antibodies because it can predict the functionality of those modifications. Moreover, when multiple

modifications are possible in a given structures, CAAD can help select the ones with best safety, efficacy, and developability balances. Therefore, the CAAD approach would potentially lead to next generation of therapeutic BsAbs with improved clinical benefits.

MATERIALS AND METHODS

Strategy for designing GB261

GB261 was designed using BioLuminate software (Schrödinger Release 2020-3: BioLuminate, Schrödinger, LLC, New York, NY, 2020. https://www.schrodinger.com/products/bioluminate.) and the design process is explained in detail in Figure 1.

Cell Lines and PBMC

Raji (Human B-lymphoma cell line, CCL-86; Lot No:63905419) and Jurkat (Human T cell lymphoblast-like cell line, Clone E6-1, TIB-152) were from ATCC. Raji cell line stably expressing GFP and Luciferase (Raji-GFP-Luciferase) was supplied by Biocytogen. They were cultured in RPMI 1640 (Thermo fisher) medium supplemented with 10% fetal bovine serum (FBS) (GIBCO) at 37°C, 5% CO_2. Human peripheral blood mononuclear cells (hPBMC) were purchased from AllCells (Alameda, CA) and HumanCells Bio (San Jose, CA). Rituximab resistant Raji cells (RRCL) were developed as described in Supplementary Materials.

Bispecific antibody purification

GB261 was produced by co-transfecting plasmids encoding the CD20 heavy chain, CD3 heavy chain and their common light chain into Expi293 cells and purified using a Protein A column on an AKTA Explorer 100 purification system and further purified using cation exchange chromatography. Detailed method is described in Supplementary materials.

Bispecific antibody cell binding assays

Binding of BsAb to CD3 and CD20 expressing cells was determined by flow cytometry. Briefly, 2×10^5 Jurkat (CD3+/CD20−) or Raji (CD20+/CD3−) cells were incubated for 30 minutes at 4 °C

with serial dilutions of BsAb or hIgG1 isotype control antibodies. Then, cells were washed with DPBS (GIBCO) containing 1% Bovine Serum Albumin (BSA) (Proliant Biologicals), and incubated with Cy3-conjugated Goat anti-human IgG (Jackson ImmunoResearch) at 1:1000 dilution for 30 minutes at room temperature (RT). The cells were washed twice, and their geometric mean fluorescence intensity (MFI) were measured using fluorescence-activated cell sorting (FACS).

In vitro cancer cell killing, T cell activation, and total T cell number assessment assays

Raji-GFP-Luc or RRCL-GFP-Luc cell were mixed with PBMC from healthy donors at ratios as indicated, plated in 96-well flat bottom plates (2.0×10^5 cell/well), treated with antibodies, and cultured in a CO_2 incubator for 48 hours. The cells were washed twice with DPBS containing 2% FBS, stained with CD69-PE (BD Biosciences) and CD2-APC (BD Biosciences) antibodies (1:100) for 45 minutes at RT, then washed twice again and analyzed using FACS. Cancer cell killing was determined by the GFP positive cell percentage, T cell activation was determined by the CD69+/CD2+ cell percentage, and total T cell number was determined by the CD2+ cell percentage.

Cytokine release Assays

The cell culture supernatants from the previous in vitro tumor cell killing, T cell activation, and total T cell number assessment assays were used for cytokine release assays. The cytokines IFN-γ, IL-2, and TNF-α were assessed using ELISA MAX Deluxe kits (BioLegend) according to manufacturer's instructions.

ADCC assays

Target cells were washed once with PBS, incubated with calcein AM (7.5 µM) at 37°C for 30 minutes in dark, washed three times with PBS, resuspended in RPMI1640 with 10% FBS (2×10^5 cells/ml) and then added to a 96-well plate (50 µl/well). Diluted antibodies (100µl) were added to each well. The plate was incubated at RT for 60 minutes, and then PBMC (effector cells) in 50 µl of media were added to each well (5×10^4 cells/well). The plate was incubated at 37°C for 4 hours

and centrifuged at 1000 rpm for 10 minutes. Supernatants were transferred into a 96-well black wall plate, and fluorescence was read at 520 nm (emission) with 485 nm excitation.

CDC assays

Target cells were labeled with calcein AM as described in ADCC assays. The labeled cells were plated in 96-well plates (1 x 10^5 cells/well in 50 µl), and antibodies at different dilutions were added (100 µl/well). The plate was incubated at RT for 15 minutes, and 10% complement-enriched human serum was added to the wells (50 µl/well). The plate was incubated at RT for 45 minutes, the cells were washed 3 times with PBS containing 0.1% BSA and stained with 7-Aminoactinomycin D (7AAD) (2 µl/well) at RT for 15 minutes in dark. The cells were analyzed by flow cytometry. The percentage of dead cells was defined as the calcein+/7AAD+ cell fraction.

Antibody-mediated cell bridging assay

Detailed method is described in Supplementary materials.

Animal Studies

All animal studies were performed in compliance with the ARRIVE guidelines.

Immediate treatment and therapeutic treatment mouse models

All animal handling, care, and treatment procedures were performed in accordance with the guidelines approved by the Institutional Animal Care and Use Committee (IACUC) of Biocytogen Boston (following the guidelines by the Association for Assessment and Accreditation of Laboratory Animal Care (AAALAC)). Nine weeks and eight weeks old female B-NDG mice (strain NOD.Cg-*Prkdc*^{scid} *Il2rg*^{tm1Bcgen}/Bcgen) (Biocytogen) were used for the immediate treatment and therapeutic treatment studies, respectively. The investigators were blinded, and only the sponsors were aware of the group allocation during each step of the experimental process.

In the immediate treatment study, the mice were randomized into 3 groups, with 4 mice per group, based on bodyweights. RRCL-GFP-Luc cells (5 x 10^5 cells/mouse) were injected with PBS into mice in the control group through i.v. administration. RRCL-GFP-Luc cells (5 x 10^5 cells/mouse) were mixed with hPBMC (5 x 10^5 cells/mouse) and either BM or GB261 and injected via the lateral

tail vein at a dose of 1.5 mg/kg at day 0. Two additional doses of antibodies were injected to mice on day 7 and day 14 as well. On day 20, the study was terminated when the mice in the control group reached humane endpoints.

In the therapeutic treatment study, RRCL-GFP-Luc cells were injected into mice (1×10^5 cells/mouse) through i.v. administration. After 3 days, the mice were divided into 3 groups at 5 mice/group. At day 4, the HLA-DR3 positive hPBMC (HumanCells Bio) were mixed with either PBS (control), BM, or GB261, and administered intravenously. Each mouse in the treatment groups received 5×10^5 hPBMC, and 20 μg of antibodies at day 0. At day 7, an additional dose of antibodies was administered to mice. On day 14, the study was terminated when the mice in the control group reached humane endpoints.

In both studies, the mice were imaged twice weekly by bioluminescence imaging (BLI), and the BLI was quantitated by the software Living Image 4.7 (Perkin Elmer). Bodyweights of mice were also measured twice a week. The mice were euthanized by CO_2 inhalation followed by a secondary physical method (such as cervical dislocation). The data were analyzed and calculated using MS Excel and GraphPad Prism 8. In the immediate and therapeutic treatment studies, the treatment and control groups were compared using unpaired T test and Kruskal-Wallis test with Dunn's multiple comparison test, respectively. A p-value of <0.05 was considered statistically significant.

Tumor relapse mouse model

All animal handling, care, and treatment procedures stated in this study were performed in accordance with the standard at Biocytogen Beijing. B-NDG mice (strain NOD.Cg-*Prkdc*^{scid} *Il2rg*^{tm1Bcgen}/Bcgen) (Biocytogen) was used for the study. Only the sponsors were aware of the group allocation and the investigators were blinded during each step of the experimental process. The mice were randomized by bodyweight into 3 groups, with 4 mice per group. Each mouse was intravenous injected with 5×10^5 Raji-Luc cells, 2.5×10^6 hPBMC, and 60 μg of antibodies (PBS for the control group). Raji-Luc cells were cultured to Logarithmic phase and the hPBMC were

thawed and incubated overnight before using for the experiments. The tumor load in mice were imaged three times weekly by BLI using IVIS Lumina LT (Perkin Elmer). Bodyweights of mice were also measured three times a week. The mice were monitored for 49 days and the study was terminated. At the study end or when the mice reached humane endpoints, they were euthanized with CO_2. The treatment and control groups were compared using unpaired T test and a p-value of <0.05 was considered statistically significant.

Cynomolgus monkey study

Before starting the experiment, the animals were raised in the experimental site for at least one week. During this period and the experimental process, the health of the animals was monitored by the veterinarian. Healthy cynomolgus monkeys (2.5-4.5 kg，3-6 years old) were randomly divided into 2 groups: 0.5 mg/kg (Group 1) and 5 mg/kg (Group 2). The investigators were not blinded and were aware of the group allocation during each step of the experimental process. Each group had two animals, including one male and one female. GB261 was administered by single-dose Intravenous infusion. Animal breeding, quarantine, drug delivery and blood collection were conducted by Laboratory of Guangxi Guidong Primate Development and Experiment Co., Ltd. (Guangxi, China) in accordance with relevant guidelines and regulations under IACUC protocol No.GD20200604 approved by the Animal Management and Use Committee of Guangxi Guidong Primate Development and Experiment Co., Ltd. The serum concentrations of GB261 and cytokines as well as percentages of T cells and B cells in blood were determined at different time points.

Data analysis

The data was analyzed by Prism (GraphPad). IC_{50} and EC_{50} values were determined using Four-parameter non-linear regression analysis.

RESULTS:

Designing process of GB261

Rituximab and a CD3 monoclonal antibody of which VL shares >80% homology to that of Rituximab were employed as two parental antibodies[23]. To develop a novel CD20/CD3 BsAb with great safety/efficacy balance as well as great manufacturability, the following features were introduced in the design process: 1) HCDR from the parental CD3 antibody were grafted in one arm of the Rituximab heavy chain; 2) CD3 binding affinity was significantly reduced to increase safety; 3) ADCC/CDC effector functions specific for cancer cells were maintained to broaden the mechanisms of action; 4) biochemical and biophysical features of the two Fv arms of the IgG-like BsAb were differentiated to facilitate better isolation of the BsAb heterodimer; 5) backmutations (CD3 HCDRs) and other modifications were introduced in the heavy chains to enhance the stability, deimmunization, and humanization; 6) new Fc mutations were introduced to improve heterodimer production and purification (Fig. 1). After designing and screening, safety, efficacy and manufacturability of the lead molecule were characterized.

GB261 has an ultra-low CD3 binding

To ensure that antibodies we designed have a good safety/efficacy balance, the binding of our redesigned CD20 and CD3 antibodies to CD20+ Raji cells and CD3+ Jurkat cells were compared with that of parental antibodies. Our redesigned CD3 antibody had a significantly lower binding to CD3+ Jurkat cells than the parental antibody, while our redesigned CD20 antibody and the parental CD20 antibody had similar binding to CD20+ Raji cells (Fig. 2A, B). Neither the redesigned nor parental CD3 antibodies had any detectable binding to Raji cells. Similarly, neither the redesigned nor parental CD20 antibodies significantly bound to Jurkat cells. Based on these studies and manufacturability data, we designed the final lead molecule, named as GB261. It had a Kd value of 1180 nM to CD3, while BM had a Kd of 9.86 nM.

The binding of GB261 to CD3+ Jurkat cells was much weaker than that of BM (Fig. 2D). However, the binding of GB261 to CD20+ Raji cells was similar to that of BM, whereas the binding of Rituximab to CD20 was much stronger that those of GB261 and BM (Fig. 2C). Moreover, both GB261 and the BM mediated bridging between Raji and Jurkat cells (Fig. 2E, F), suggesting a mechanism by which the antibodies mediate cancer cell killing.

GB261 has balanced safety/efficacy *in vitro*

To compare the effects of GB261 and BM on T cell activation, Jurkat cells were co-cultured with Raji (CD20+) cells at a ratio of 1:1, treated with different concentrations of antibodies, and then stained with anti-human CD69-PE antibody and analyzed using FACS. In the presence of Raji cells, both GB261 and BM induced a dose-dependent effect on the Jurkat cell activation, but GB261 was less efficient than the BM in Jurkat cell activation (Fig 3A, left). GB241, a biosimilar of Rituximab, and an isotype control antibody, which has similar Fc segment to GB261 but does not have a relevant Fab segment, did not induce Jurkat cell activation. Moreover, GB261 did not activate Jurkat cells in the presence of CD20- cells, whereas BM activated Jurkat cells at high concentrations due to its stronger binding to CD3 (Fig. 3A, middle). In addition, GB261 did not induce Jurkat cell activation in the presence of NK92-CD16 cells, suggesting that GB261 cannot induce T cell activation through Fc/FcR interaction (Fig. 3A, right). These data suggest that GB261 may have better safety than the BM.

To compare the Fc effector functions of GB261 and Rituximab, ADCC and CDC assays were performed. At low concentrations, GB261 was less effective than Rituximab analog and CD20 homodimer antibody in eliciting ADCC on CD20+ Raji cells, whereas at high concentrations, GB261 exhibited similar effect to Rituximab analog and CD20 homodimer antibody (Fig. 3B, up). Similar results were observed in CDC assays (Fig. 3C, up). These antibodies did not induce ADCC or CDC on CD20- Jurkat cells (Fig. 3B, C, lower). In other words, GB261 only induced ADCC and CDC on CD20+ cells, but not on CD3+ T cells, suggesting its good safety/efficacy balance.

To compare the effects of GB261 and BM on cancer cell killing, T cell activation and total T cell number in Rituximab-resistant cells, RRCL-GFP-Luc cells were incubated with hPBMCs either at 1:1 ratio or 1:4 ratio in the presences of different concentrations of testing antibodies. At 48 hours post-incubation, GFP+ cell surviving percentage, T cell activation, and total T cell number were detected, respectively. As shown in Fig. 4, GB261 and BM had similar effects on RRRC killing (A), T cell activation (B) and total T cell number (C), showing the efficacy of GB261.

Immunotherapy can cause CRS when immune cells are activated and release large amounts of cytokines into the body [24,25]. High levels of cytokines can result in increased inflammation. Thus, they can be harmful and cause organ failure and even death [26]. Therefore, a successful immunotherapeutic antibody should be able to induce T cell activation and cancer cell killing but not elicit a strong CRS. To this end, we compared the effects of GB261 and BM on the release of several cytokines. GB261 induced less IL-2, IFNγ and TNFα secretion than BM, suggesting that GB261 has less potential to induce CRS (Fig. 4D).

GB261 retains favorable efficacy at low T/B cell ratios *in vitro* and *in vivo*

Previous studies have shown that when cancer B cells overgrow in patients, the B/T cell ratio could significantly increase [27]. Therefore, we analyzed whether GB261 with Fc effector functions is better than the Fc-silenced BM in low T/B cell ratios due to initial cancer cell elimination and T/B ratio re-adjustment by ADCC and/or CDC. To do so, we performed *in vitro* and *in vivo* studies comparing cancer killing by GB261 and BM at different T/B ratios. GB261 was more efficacious than BM when PBMC/RRCL and PBMC/Raji cell ratios were low *in vitro* (Fig. S1). To compare this effect *in vivo*, RRCL-GFP-Luc cells were i.v. injected into female B-NDG mice, and after 3 days, the mice were randomly divided into 3 groups. At day 4, together with PBMC, the first group were i.v. administered with PBS, second group with BM, and the third group with GB261. Although both BM and GB261 induced RRCL killing in PBMC-engrafted mice, GB261 was much more effective than BM, and both antibodies induced comparable body weight change in mice (Fig. 5C). However, in another study, when RRCL cells were injected with PBMC and antibodies at

the same time (lower luciferase signal implies higher effector/target cell ratio at the beginning of the study), GB261 and BM had similar effects on tumor size decrease and body weight in mice (Fig. 5B). The significant increase in the number of RRCL cells when they are injected 4 days before antibody treatment, as shown by the day 3 (post-antibody treatment) luminescence signal increase compared to when RRCL and antibodies are injected together (Data not shown), decreases the T cell/RRCL ratio, thus reducing BM efficacy, whereas GB261 can increase the T cell/RRCL ratio via ADCC/CDC, consequently retaining its efficacy. This is likely due to the increased T cell activation when the T cell/cancer cell ratios are higher, as demonstrated by our *in vitro* data (Fig. 5A).

To compare the efficacies of GB261 and Rituximab in lymphoma cell killing, RRCL-GFP-Luc were treated with PBS, GB261, and Rituximab analog, respectively, mixed with PBMCs, and then i.v. injected into female B-NDG mice. Raji cell proliferation was monitored using luciferase imaging. GB261 effectively mediated Raji cell killing through the whole experimental period. Rituximab analog also effectively mediated Raji cell killing during the initial 16 days, but it lost its Raji cell killing capacity after the initial period (Fig. 6). These data suggest that GB261 but not Rituximab mediate the killing of relapsed lymphoma.

GB261 has good safety in cynomolgus monkeys

Next, we determined whether GB261 treatment depletes circulating B cells and whether it causes any unexpected toxicity in cynomolgus monkeys. The animals were treated with either 0.5 or 5 mg/kg of GB261, and levels of circulating B cells, T cells and inflammatory cytokines were monitored for 8 weeks. After infused with different doses of GB261, CD20+ cells (B cells) were depleted rapidly, and CD20+ could not be detected after 24 hours. With the extension of monitoring time, CD20+ recovered to a certain extent (Fig. 7A). The CD3+ T cells increased to a certain extent and remained higher than the levels before administration after 56 days (Fig. 7B). In addition, there was no significant amounts of cytokines detected except for IL-6. This is probably caused by the significantly lower binding of GB261 to cynomolgus CD3 compared to its

binding to human CD3 (Fig. 2D, 7C and 7D). Together with our in vitro data, these data suggest that GB261 also exhibits great safety/efficacy balance in primates.

GB261 has favorable manufacturability features

GB261 has a good expression in CHO cells (~6g/L). The heterodimer formation percentage is high which enables its high-efficient production (Fig. S2A). In addition, the product has a good purity (Fig. S2B, C), aggregation resistance, and thermostability (Fig. S2D).

DISCUSSION

While the discovery of therapeutic antibody candidates is a relatively straightforward process, their development to clinically approved drugs often confront with unexpected problems. In this study, we present that GB261, a novel CD20/CD3 BsAb designed from Rituximab, retains Fc effector function that only targets B cells and gains T cell engager function with reduced CRS. CRS is a major problem frequently associated with T cell engagers[24,25]. Previous studies have shown that cytokine release is dependent on the binding affinity of the CD3 binding arm [28,29]. To reduce CRS, GB261 was designed to have reduced CD3 binding to overcome potential safety issues caused by extra T cell activation.

Compared with a benchmark CD20/CD3 BsAb, GB261 has a low CD3 binding affinity (Fig. 2), which enables GB261 to activate T cells in the presence of CD20+ target tumor cells, but not in their absence. Also, the ultra-low CD3 binding of GB261 minimizes the ADCC/CDC-mediated T cell killing caused by the Fc/FcR interactions but retains ADCC/CDC mediated B cell killing.

Although GB261 elicits less cytokine release compared to BM, it does not compromise its efficacy. In fact, it retains T cell activation and cancer killing capacity on Rituximab resistant Raji cells comparable to that of BM. Furthermore, the cancer cell killing capacity of GB261 is comparable to that of BM at higher T/B cell ratios, but higher than that of BM at lower T/B cell ratios that mimics the pathophysiological conditions. This high efficacy of GB261 at low T/B cell ratios can be

attributed to its multiple mechanisms of action (MOA). GB261 can target cancer cells via Fc effector functions ADCC/CDC/ADCP, or T cell-mediated killing. At initial stage of treatment when the B cancer cells are more prevalent than T cells, GB261 can eliminate cancer cells via Fc effector functions with the aid of NK cells, macrophages (M), and the complement pathway. This would reduce the cancer cell numbers and result in higher T/B cell, NK/B cell, and M/B cell ratios. Therefore, at later stages of the treatment, the T cell-mediated B cell killing would be more prominent because this action is more efficient at higher T/B cell ratios where the T cells are activated more efficiently. The increased NK/B and M/B cell ratios would further enhance the Fc-mediated elimination of cancer cells at later stages of the treatment, assisting the action of T cell-mediated B cancer cell killing (Fig. 7E). This is further supported by the observation that GB261 inhibited cancer cell growth at low doses, in a dosing study *in vivo* (Fig. S3). For antibodies without Fc effector functions, additional agents with Fc effector functions might initially be required to increase the T/B cell ratio. This is the reason that REGN1979 is more efficient when Rituximab is used to increase the T/B cell ratio before REGN1979 administration [30]. Later on, when most cancer B cells are killed, there are more free T cells which could still be activated by BM but not GB261 (Fig.1). This assertation is supported by both our in vitro data and the mouse models, where GB261 shows superior cancer cell killing than BM in a PBMC engrafted mouse model if RRCL cells were injected first, then PBMC cells and antibodies were co-injected 4 days later when the T/B cell ratio is decreased in animals. In contrast, GB261 exhibits similar cancer killing effect to BM when RRCL and PBMC cells were co-injected with antibodies when the T/B cell ratio is relatively high.

These multiple MOA enable GB261 to counter the drug resistance of cancer cells better than agents with a single MOA. Cancers are comprised of heterogenous cell populations in terms of both therapeutic response (Ex: cells with diverse mutations) and resistance development. Therefore, GB261 has the ability to clear the residual cancer cell populations that might survive the treatment with a drug with a single MOA, thereby enhancing cancer clearance. In addition,

GB261 can counter different modes of drug resistance development in cancer cells due to its multiple MOA compared with a single MOA agent. These drug resistance mechanisms include but not limited to PD-L1/PD-1 overexpression to reduce T cell activation [31], CD46/CD55/CD59 overexpression to inhibit CDC [32] and CD16A ***V*** & ***F*** genotypes to affect ADCC [33]. This decreases the chance of cancer relapse in patients. This is exemplified by our in vivo studies that shows GB261 does not cause cancer relapse for the entire duration of the study, whereas a Rituximab analog causes relapse after decreasing the cancer burden initially (Fig. 6).

GB261 exhibits a favorable manufacturability. It has good expression, and a high heterodimer/homodimer formation ratio. Also, the product is easily purified with good yield and purity. In addition, the purified antibody has a good thermostability and is aggregation resistant. The results suggest that GB261 would meet the Chemistry Manufacturing and Controls (CMC) requirements for successful drug development. Taken together, GB261 has a good balance among efficacy, safety, and developability, and has the potential to replace Rituximab as a first-line drug in lymphoma therapy.

DATA AVAILABILITY

For original data, please contact yue.liu@antibodystudio.com.

REFERENCES

1 Ventola, C. L. Cancer Immunotherapy, Part 3: Challenges and Future Trends. *P T* **42**, 514-521 (2017).

2 Esfahani, K. *et al.* A review of cancer immunotherapy: from the past, to the present, to the future. *Curr Oncol* **27**, S87-S97, doi:10.3747/co.27.5223 (2020).

3 Waldman, A. D., Fritz, J. M. & Lenardo, M. J. A guide to cancer immunotherapy: from T cell basic science to clinical practice. *Nature Reviews Immunology* **20**, 651-668, doi:10.1038/s41577-020-0306-5 (2020).

4 June, C. H. *et al.* Engineered T cells for cancer therapy. *Cancer Immunol Immunother* **63**, 969-975, doi:10.1007/s00262-014-1568-1 (2014).

5 Hong, M., Clubb, J. D. & Chen, Y. Y. Engineering CAR-T Cells for Next-Generation Cancer Therapy. *Cancer Cell* **38**, 473-488, doi:https://doi.org/10.1016/j.ccell.2020.07.005 (2020).

6 Couzin-Frankel, J. Cancer Immunotherapy. *Science* **342**, 1432-1433, doi:10.1126/science.342.6165.1432 (2013).

7 Weiner, L. M., Dhodapkar, M. V. & Ferrone, S. Monoclonal antibodies for cancer immunotherapy. *Lancet* **373**, 1033-1040, doi:10.1016/S0140-6736(09)60251-8 (2009).

8 Wu, Z. & Cheung, N. V. T cell engaging bispecific antibody (T-BsAb): From technology to therapeutics. *Pharmacology & Therapeutics* **182**, 161-175, doi:https://doi.org/10.1016/j.pharmthera.2017.08.005 (2018).

9 Cao, Y. *et al.* Multiformat T-cell-engaging bispecific antibodies targeting human breast cancers. *Angew Chem Int Ed Engl* **54**, 7022-7027, doi:10.1002/anie.201500799 (2015).

10 Goebeler, M.-E. & Bargou, R. C. T cell-engaging therapies — BiTEs and beyond. *Nature Reviews Clinical Oncology* **17**, 418-434, doi:10.1038/s41571-020-0347-5 (2020).

11 Trabolsi, A., Arumov, A. & Schatz, J. H. T Cell–Activating Bispecific Antibodies in Cancer Therapy. *The Journal of Immunology* **203**, 585-592, doi:10.4049/jimmunol.1900496 (2019).

12 Einsele, H. *et al.* The BiTE (bispecific T-cell engager) platform: Development and future potential of a targeted immuno-oncology therapy across tumor types. *Cancer* **126**, 3192-3201, doi:https://doi.org/10.1002/cncr.32909 (2020).

13 Wu, J., Fu, J., Zhang, M. & Liu, D. Blinatumomab: a bispecific T cell engager (BiTE) antibody against CD19/CD3 for refractory acute lymphoid leukemia. *J Hematol Oncol* **8**, 104-104, doi:10.1186/s13045-015-0195-4 (2015).

14 Slaney, C. Y., Wang, P., Darcy, P. K. & Kershaw, M. H. CARs versus BiTEs: A Comparison between T Cell–Redirection Strategies for Cancer Treatment. *Cancer Discovery* **8**, 924-934, doi:10.1158/2159-8290.Cd-18-0297 (2018).

15 Smith, E. J. *et al.* A novel, native-format bispecific antibody triggering T-cell killing of B-cells is robustly active in mouse tumor models and cynomolgus monkeys. *Sci Rep* **5**, 17943-17943, doi:10.1038/srep17943 (2015).

16 Sun, L. L. *et al.* Anti-CD20/CD3 T cell–dependent bispecific antibody for the treatment of B cell malignancies. *Science Translational Medicine* **7**, 287ra270-287ra270, doi:10.1126/scitranslmed.aaa4802 (2015).

17 Bannerji, R. *et al.* Phase 1 Study of REGN1979, an Anti-CD20 x Anti-CD3 Bispecific Monoclonal Antibody, in Patients with CD20+ B-Cell Malignancies Previously Treated with CD20-Directed Antibody Therapy. *Blood* **128**, 621-621, doi:10.1182/blood.V128.22.621.621 (2016).

18 Gin, G. A., Anca. (Affimed, 2018).

19 Idrus, A. A. (ed Amirah Al Idrus) (Fierce Biotech, Fierce Biotech, 2019).

20 Carroll, J. *Endpoints News* (ed John Carroll) (Carroll, John, Endpoints News, 2019).

21 Cartron, G., Watier, H., Golay, J. e. & Solal-Celigny, P. From the bench to the bedside: ways to improve rituximab efficacy. *Blood* **104**, 2635-2642, doi:10.1182/blood-2004-03-1110 (2004).

22 Boross, P. & Leusen, J. H. W. Mechanisms of action of CD20 antibodies. *Am J Cancer Res* **2**, 676-690 (2012).

23 LIU, Y., CAI, W. & SHI, J. WO2019028125 - BISPECIFIC ANTIBODIES AND USES THEREOF. United States patent WO/2019/028125 (2019).

24 Shimabukuro-Vornhagen, A. *et al.* Cytokine release syndrome. *J Immunother Cancer* **6**, 56-56, doi:10.1186/s40425-018-0343-9 (2018).

25 Murthy, H., Iqbal, M., Chavez, J. C. & Kharfan-Dabaja, M. A. Cytokine Release Syndrome: Current Perspectives. *Immunotargets Ther* **8**, 43-52, doi:10.2147/ITT.S202015 (2019).

26 Lee, D. W. *et al.* Current concepts in the diagnosis and management of cytokine release syndrome. *Blood* **124**, 188-195, doi:10.1182/blood-2014-05-552729 (2014).

27 Golay, J. *et al.* Biologic response of B lymphoma cells to anti-CD20 monoclonal antibody rituximab in vitro: CD55 and CD59 regulate complement-mediated cell lysis. *Blood* **95**, 3900-3908 (2000).

28 Ferran, C. *et al.* Cytokine-related syndrome following injection of anti-CD3 monoclonal antibody: further evidence for transient in vivo T cell activation. *Eur J Immunol* **20**, 509-515, doi:10.1002/eji.1830200308 (1990).

29 Zlabinger, G. J. *et al.* Cytokine release and dynamics of leukocyte populations after CD3/TCR monoclonal antibody treatment. *J Clin Immunol* **12**, 170-177, doi:10.1007/bf00918085 (1992).

30 Brownstein, C. M. *et al.* First-in-human study assessing safety and tolerability of REGN1979, a novel CD20xCD3 bispecific antibody, in patients with CD20+ B-cell malignancies previously treated with anti-CD20 therapy. *Journal of Clinical Oncology* **33**, TPS3089-TPS3089, doi:10.1200/jco.2015.33.15_suppl.tps3089 (2015).

31 Riley, J. L. PD-1 signaling in primary T cells. *Immunol Rev* **229**, 114-125, doi:10.1111/j.1600-065X.2009.00767.x (2009).

32 Geis, N. *et al.* Inhibition of Membrane Complement Inhibitor Expression (CD46, CD55, CD59) by siRNA Sensitizes Tumor Cells to Complement Attack In Vitro. *Current Cancer Drug Targets* **10**, 922-931, doi:http://dx.doi.org/10.2174/156800910793357952 (2010).

33 Sung, A. P. *et al.* An improved method to quantify human NK cell-mediated antibody-dependent cell-mediated cytotoxicity (ADCC) per IgG FcR-positive NK cell without purification of NK cells. *Journal of Immunological Methods* **452**, 63-72, doi:https://doi.org/10.1016/j.jim.2017.11.002 (2018).

ACKNOWLEDGEMENT

The authors would like to thank all contributors of this project for their opinions and support in this study.

AUTHOR CONTRIBUTIONS

Wenyan Cai performed cell-based assays, designed some animal studies, analyzed data and contributed to drafting of the manuscript. Jianbo Dong designed antibody engineering work, performed the experiments, and analyzed data. Sachith Gallolu Kankanamalage designed some cell-based assays, performed experiments, analyzed data and prepared manuscript. Allison Titong designed some cell-based assays and analyzed data. Bo Wang developed the purification strategy of bispecific antibody. Jiadong Shi designed some cell-based assays, performed experiments, and analyzed data. Zhejun Jia performed molecular cloning work. Cai Huang analyzed data and prepared manuscript. Jing Zhang designed the cyno pre-tox study, Jun Lin, Steven Z. Kan led the CMC process and produced GB261, Joe Zhou led all research at Genor Biopharma, analyzed the data and revised the manuscript. Yue Liu conceived the idea, designed GB261 molecule, analyzed the data and prepared manuscript.

COMPETING INTERESTS

Wenyan Cai is a former employee of Ab Studio Inc. and currently works at Genor Biopharma Co. Ltd. Jianbo Dong, Sachith Gallolu Kankanamalage, Allison Titong, and Bo Wang are employees of Ab Studio Inc. Jiadong Shi and Zhejun Jia are former employees at Ab Studio Inc. Cai Huang is an employee at Ab Therapeutics Inc. Jing Zhang, Jun Lin, Steven Z. Kan, and Joe Zhou are employees of Genor Biopharma Co. Ltd. Yue Liu is the Founder of Ab Studio Inc. and Ab Therapeutics Inc. Ab Studio Inc., Ab Therapeutics Inc., and Genor Biopharma Co. Ltd. are actively engaged in the commercial development of therapeutic antibodies.

FUNDING

This study was conducted by research funding from Ab Studio Inc. and Genor Biopharma Co. Ltd., a JHBP company.

FIGURE LEGENDS

Figure 1. Computer aided design process of the "imbalanced" BsAb GB261. HCDRs in one arm of the parental CD20 (Rituximab) was replaced by the HCDRs of parental CD3 antibody to construct the preliminary CD20/CD3 BsAb. Several common VL sequences that share homology to VL (CD20) and VL (CD3), and may lead to loss of binding to CD3 but maintains binding to CD20 were designed and paired with the two VHs. These IgG like BsAbs with different common VL candidates were constructed in the "knob into hole (KIH)" format. Then, T cell activation assays were performed to select the lead BsAb molecule with the best safety/efficacy balance. Then, new mutations in the Fc domain were introduced to further improve heterodimer formation. In addition, the pI of the two BsAb VHs were differentiated by introducing new mutations in the VH non-CDR framework regions. The deimmunization mutations were also introduced. The final lead molecule，GB261 v4b was selected based on

great safety/efficacy balance as well as great manufacturability represented by high expression level, high heterodimer formation percentage, easy purification process, and great biochemical and biophysical characterization data.

Figure 2. GB261 is much weaker than BM in CD3 binding but is comparable in CD20 binding. A) Binding of designed CD20 and CD3 antibodies to CD20+ Raji cells, compared with those of the parental CD20 and CD3 antibodies. Cells were incubated with antibodies, labeled with Cy3-conjugated Goat anti-human antibody, followed by FACS. The binding was presented as the percentage of cells positive for staining. B) Antibodies tested in Fig. 2A were examined for binding to CD3+ Jurkat cells using the same method. C) Binding of GB261, BM and Rituximab analog to Raji cells. The cells were labeled with a Cy3-conjugated Goat anti-human antibody and analyzed using FACS. The binding was quantified as the mean fluorescent intensity (MFI) of staining. D) Binding of GB261 and BM to Jurkat cells. E) Raji-GFP cells were mixed with Jurkat cells pre-stained with CellVue Claret Far Red fluorescent dye at 1:1 ratio and incubated overnight with 20 μg/ml antibodies, followed by the detection of cells by FACS. The events double positive for GFP and fluorescent dye were counted as bridged Raji-GFP and Jurkat cells. F) Raji-GFP cells were mixed with unstained Jurkat cells at 1:1 ratio, incubated with 20 μg/ml antibodies, and stained with DyLight 594-conjugated goat anti-human IgG. Two representative images showing the bridging of Raji-GFP cells and Jurkat cells in the presence of antibodies are shown. The display of the images has been adjusted non-uniformly for representation.

Figure 3. GB261 has balanced safety/efficacy. A) Jurkat (T cell) activation by GB261, BM, GB241, and an isotype IgG as performed by co-incubating with Raji (left), CHO cells (middle) and NK92-CD16 cells (right) at 1:1 ratio. The cells were labeled with anti-CD69 antibodies conjugated to PE and analyzed by flow cytometry. B) Upper panel, ADCC induced by either GB261, an anti-CD20 homodimer, Rituximab analog, or an isotype IgG. Raji cells labeled with Calcein AM were treated with antibodies and incubated with NK-92-CD16 cells. Lower panel examines whether the GB261-induced ADCC kills T cells that it binds to. Human PBMC were

incubated with GB261, Rituximab analog, a CD3 mAb, and the isotype control antibody. T cell viability was analyzed by FACS. C) Upper panel, CDC induced by either GB261, a CD20 homodimer, Rituximab analog, or an isotype IgG. Raji cells labeled with Calcein AM were treated with antibodies and incubated with complement-enriched human serum. Lower panel, Jurkat cells were incubated with antibodies as described in C Upper panel and the viability of the cells were analyzed by FACS.

Figure 4. GB261 and BM has similar effects on tumor cell killing, T cell activation and total T cell number, but GB261 induces less cytokine release compared to BM. hPBMC were mixed with RRCL-GFP-Luc cells at E:T 1:1 or 4:1 ratios and incubated with test antibodies GB261 and BM, or an isotype control antibody for 48 hours. The cells were labeled with CD2-APC and CD69-PE antibodies followed by analyzing with FACS. A) RRCL-GFP-Luc killing was assessed by the percentage of survived GFP positive cells. B) T cell activation was determined by the percentage of CD2+/CD69+ cells, and C) total T cell number was assessed by the percentage of CD2+ cells. D) The experiment was performed as described above, and the release of cytokines was detected by ELISA using the cell culture supernatants.

Figure 5. GB261 has better efficacy compared to the BM at low T/B cell ratios. A) hPBMC and Raji-GFP-Luc cells were mixed at ratios of 1:1, 1:3 and 1:9 and incubated with indicated concentrations of GB261 or an isotype IgG. T cell activation was assessed by measuring CD69+/CD2+ T cells by FACS. The background T cell activation by the isotype control antibody was subtracted from the values obtained for GB261. B) RRCL-GFP-Luc cells were mixed with HLA matching (HLA-DR3+) hPBMC at 1:1 ratio. Then, the cells were mixed with PBS, GB261, or BM, and subsequently injected into mice by i.v. (4 mice/group). Each mouse received 5 x 10^5 RRCL-GFP-Luc cells and 5 x 10^5 PBMC, with or without the antibodies. An amount of 20 µg of antibodies were administered at day 0 and day 7, and 60 µg of antibodies were administered at day 14. The mice were monitored for a total period of 21 days and the tumor luminescence was imaged every 3 days. The workflow, total tumor luminescence on Day 20, and the percentage

body weight change of the mice from the initial weight are shown in the upper, lower left, and lower right panels, respectively. C) The mice were first inoculated by RRCL-GFP-Luc cells. After 4 days, the HLA matching hPBMC were mixed with PBS (Control) or 1 mg/kg test antibodies GB261 or BM, and injected into mice by i.v (5 mice/group). At this point, the T:B cell ratio is about 1:8. Each mouse received 5 x 10^5 RRCL-GFP-Luc cells and 5 x 10^5 PBMC. The antibodies were administered at day 0 and day 7 and the mice were monitored for a total period of 14 days. The tumor luminescence was imaged every 3 days. The workflow, total tumor luminescence on Day 14, and the percentage body weight change of the mice from the initial weight are shown in the upper, lower left, and lower right panels, respectively.

Figure 6. GB261 prevents tumor relapse in an in-vivo mouse model. Raji-GFP-Luc cells and hPBMC were mixed with either PBS, GB261, or Rituximab, and injected into mice by i.v. A total of 4 animals were used per each treatment group. The mice received 5 x 10^5 Raji-GFP-Luc cells, 2.5 x 10^6 PBMC, and 60 μg of each antibody. They were imaged for the tumor luminescence at 15 minutes post-i.v., and then at day 2, day 3 and every 3 days after that. The mice were monitored for a total period of 31 days. The tumor volume was quantified (A) and the luminescent images of the mice are shown (B).

Figure 7. Effects of GB261 on CD20+ and CD3+ lymphocytes in Cynomolgus monkeys. A) CD20+ lymphocytes and GB261 levels in Cynomolgus monkey blood after administration of 0.5 mg/ml or 5 mg/ml of GB261. Lymphocytes are mean of 2 Cynomolgus monkeys. GB261 levels are mean of 9 Cynomolgus monkeys. B) CD3+ lymphocytes of Cynomolgus monkeys after administration of 0.5 mg/ml or 5 mg/ml of GB261. Data are mean of 2 Cynomolgus monkeys. C) The binding of GB261 or an isotype control antibody at indicated concentrations to recombinant human, Cynomolgus, and mouse CD3D and E heterodimers were assessed by ELISA. The binding was measured as the optical density (OD) values at 450 nm and 570 nm. D) Binding of CD3 homodimer and an isotype control antibody to Cynomolgus PBMC, determined by FACS. E) A model depicting the mechanisms of action of GB261, compared with those of BM.

FIGURES

Figure 1

Figure 1

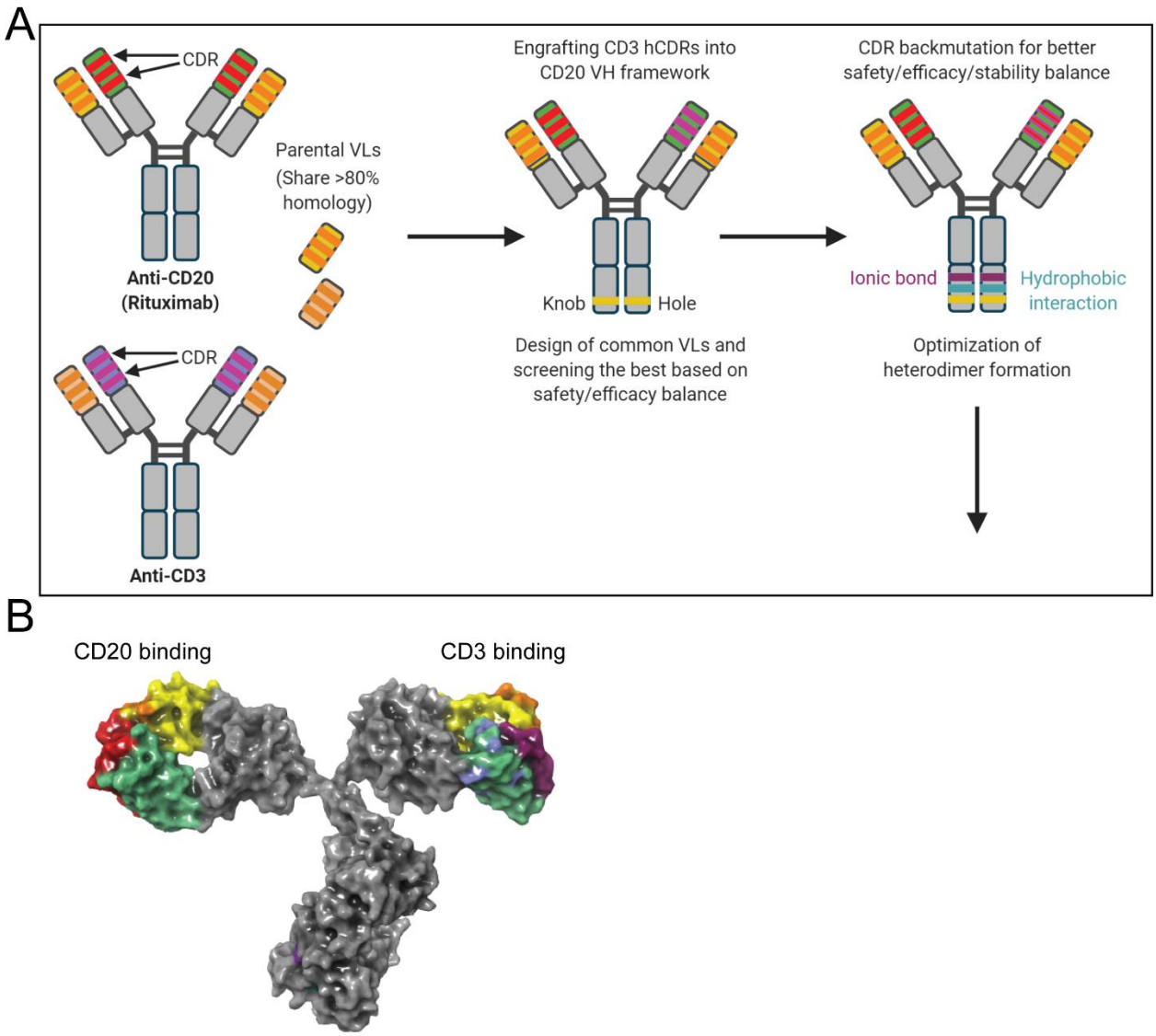

Figure 2

Figure 2

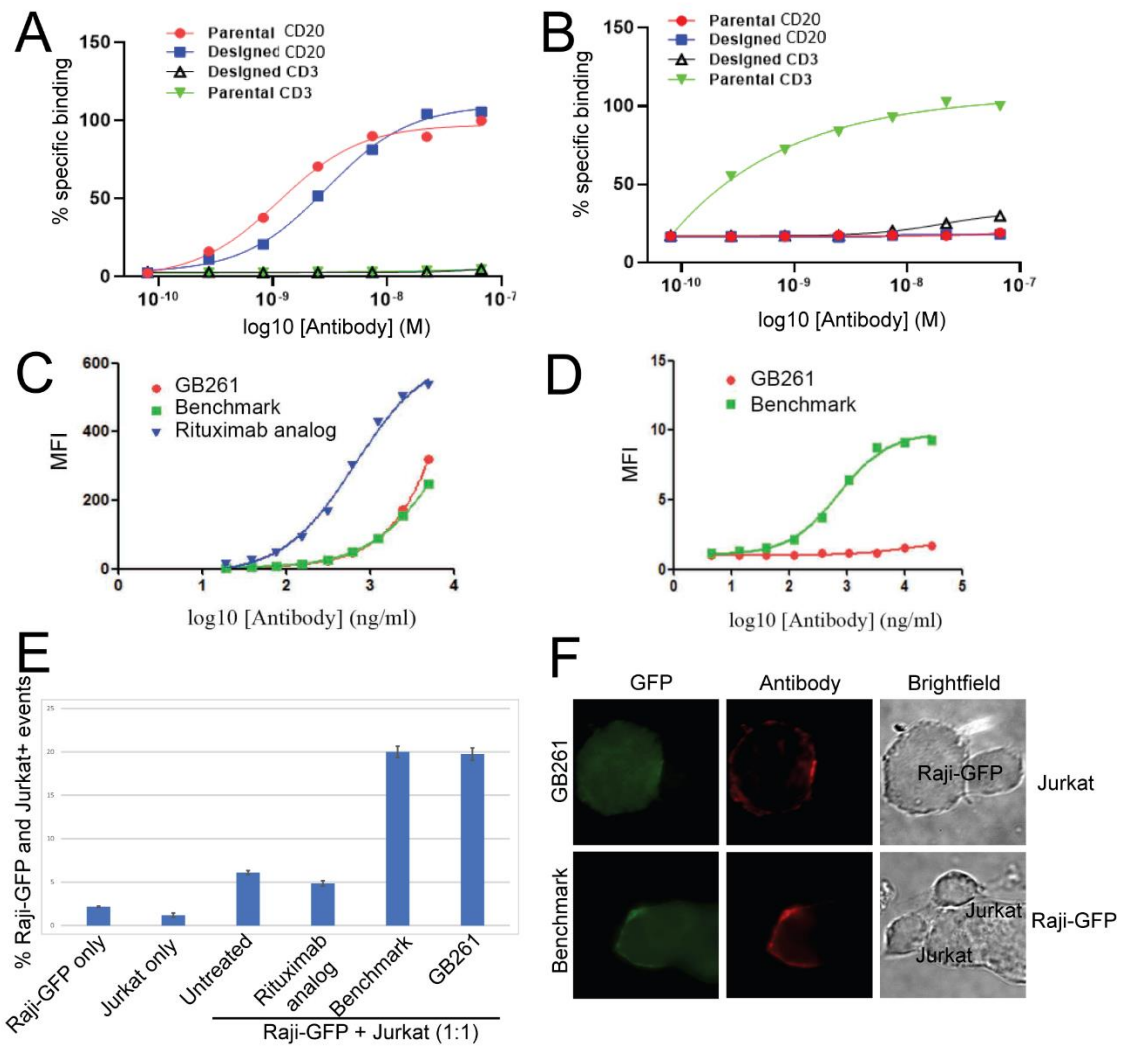

Figure 3

Figure 3

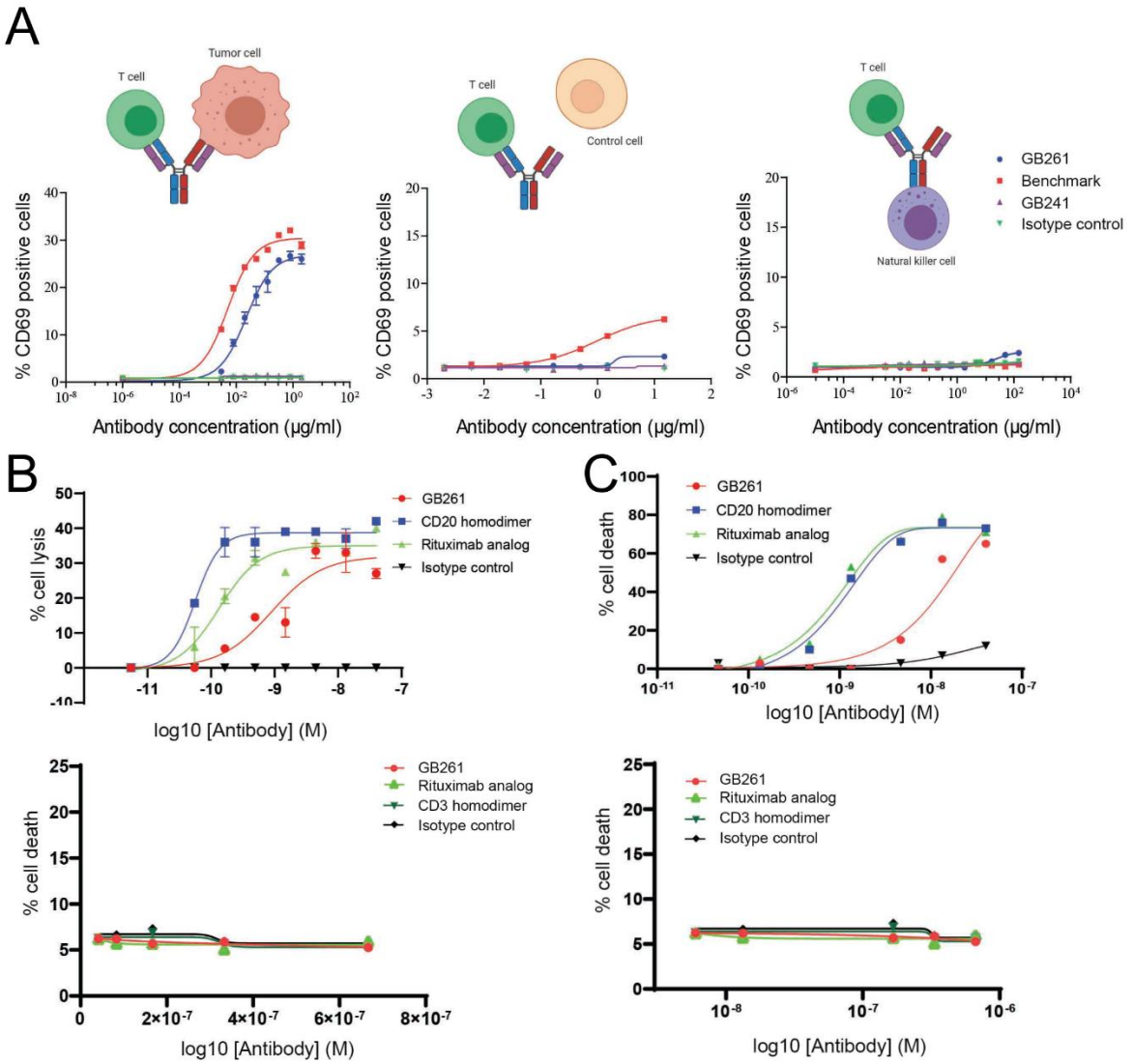

Figure 4

Figure 4

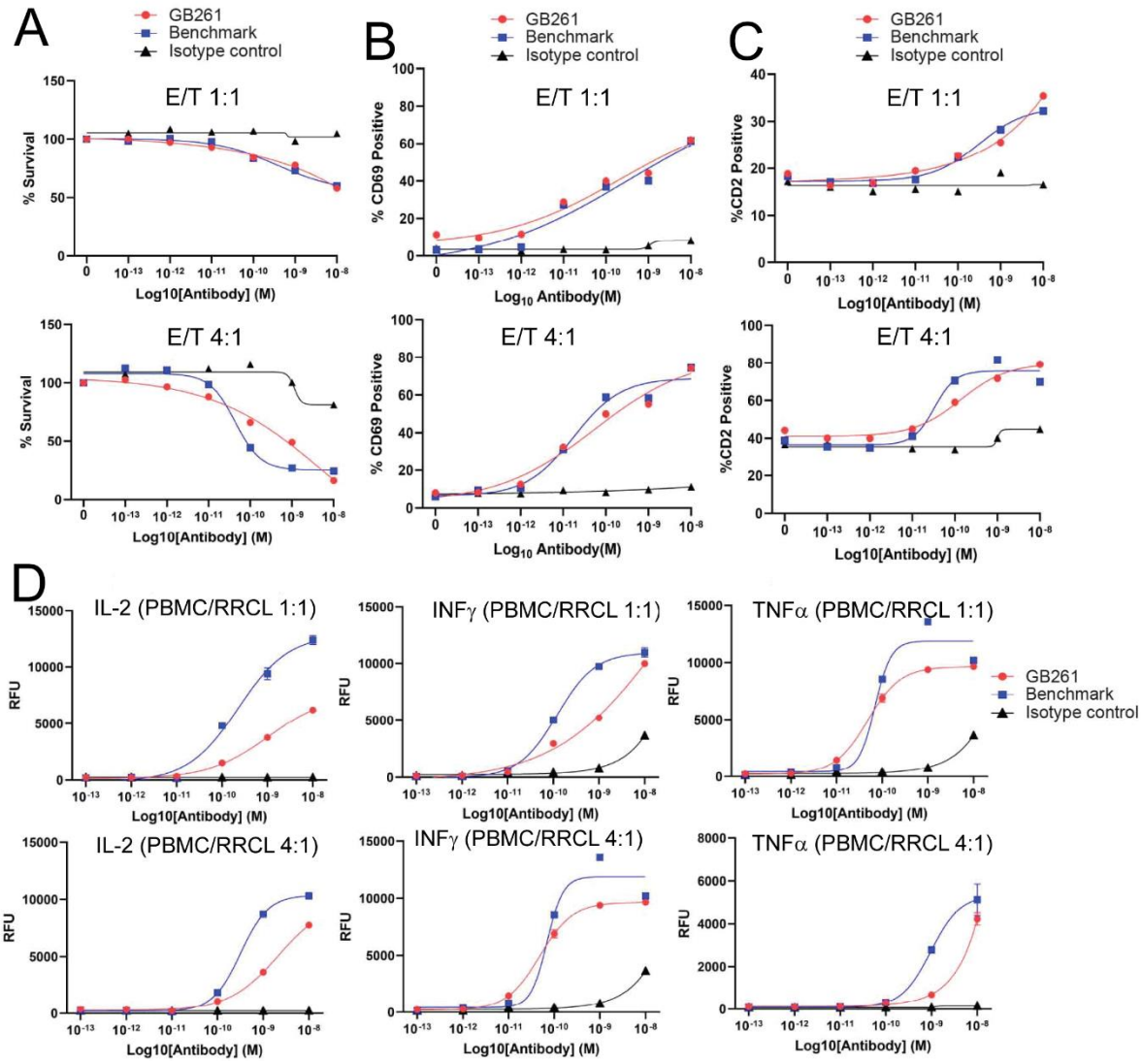

Figure 5

Figure 5

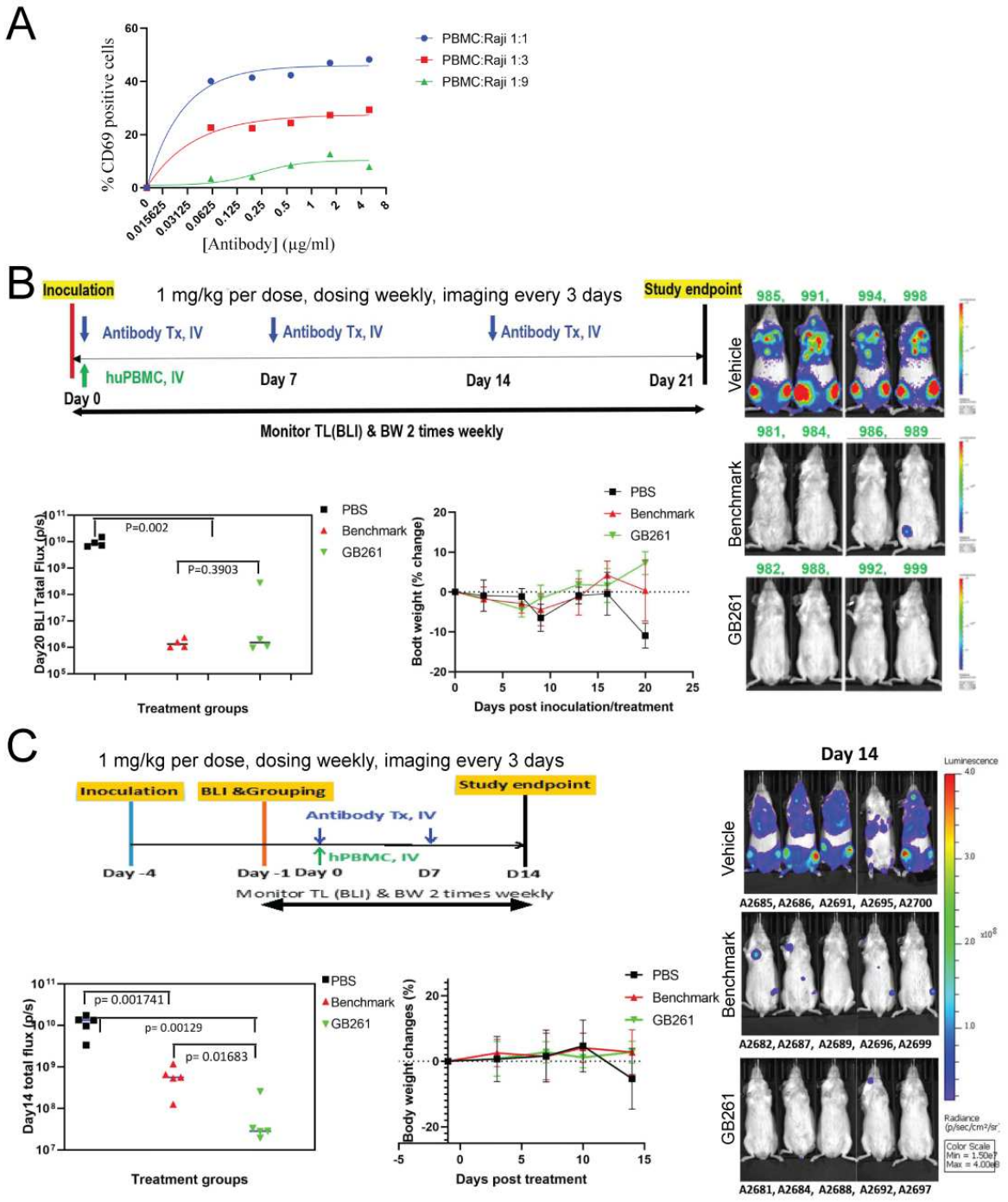

Figure 6

Figure 6

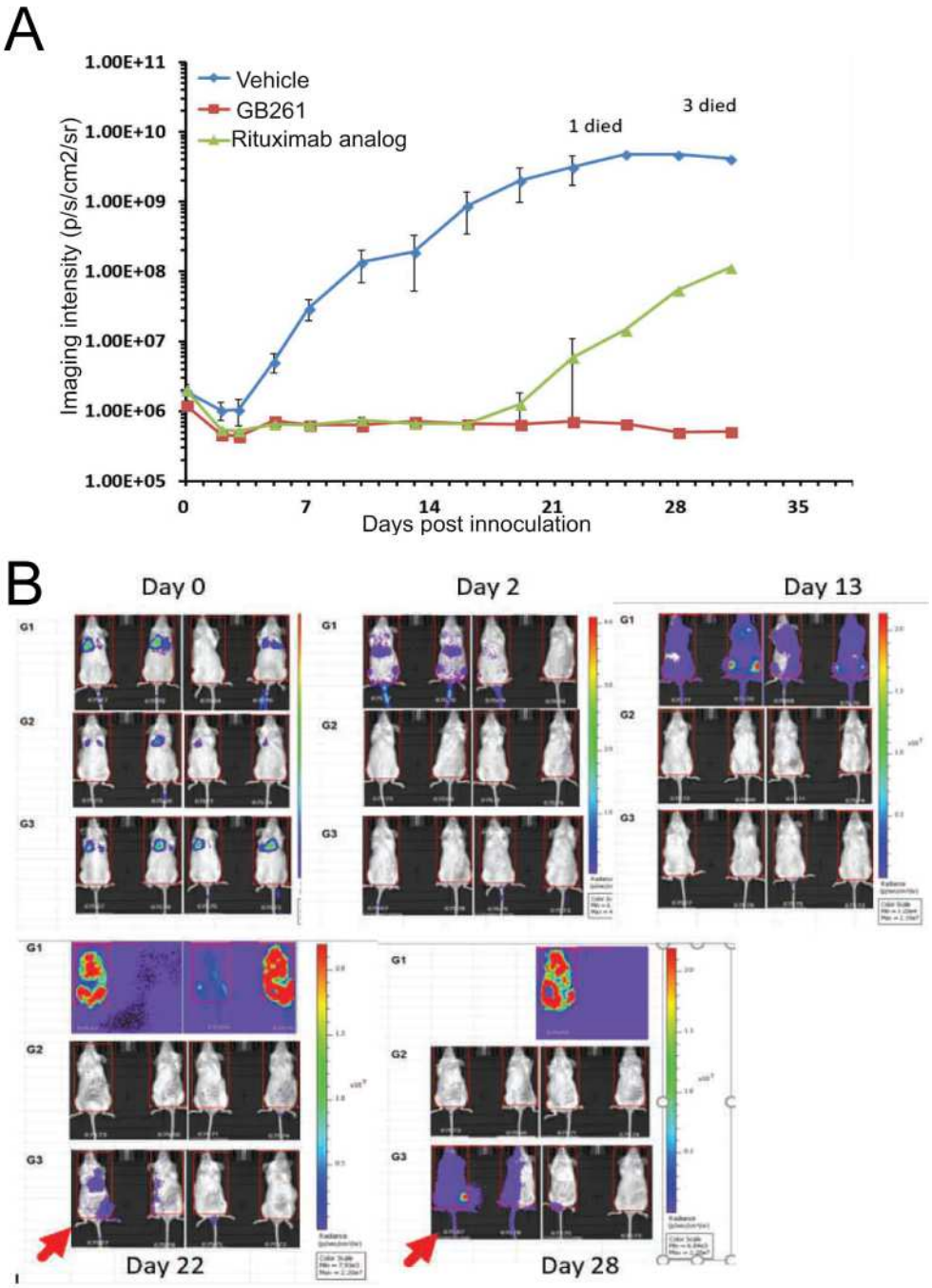

644 **Figure 7**

Figure 7

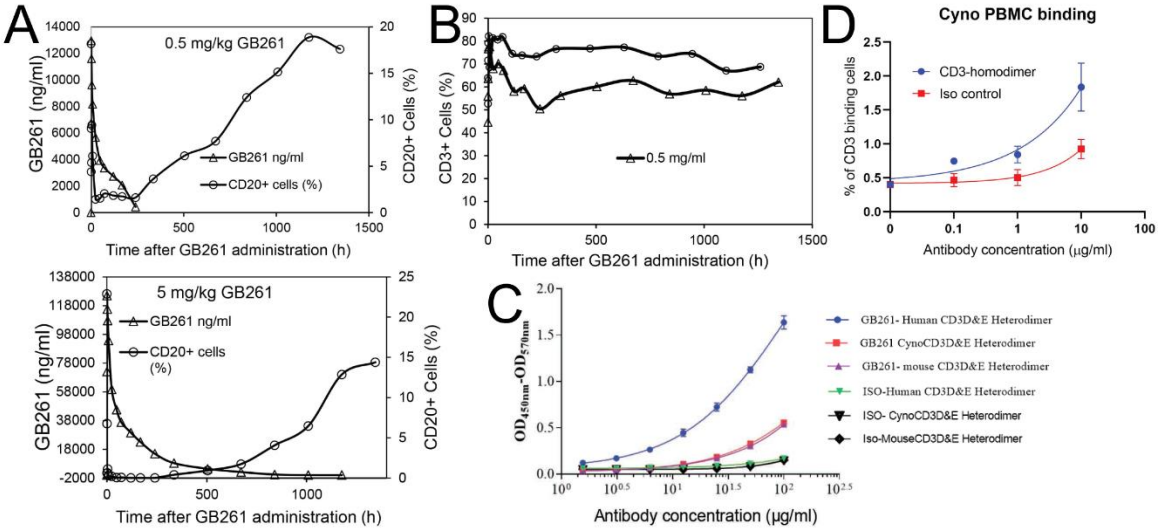

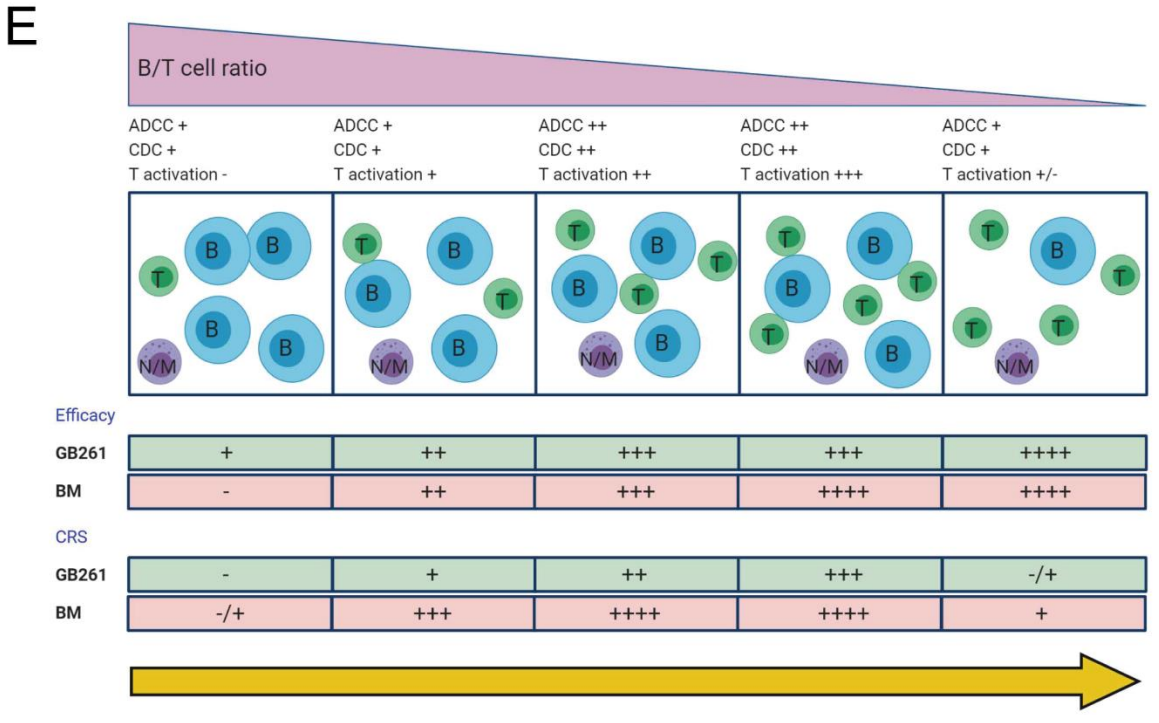

645

Figures

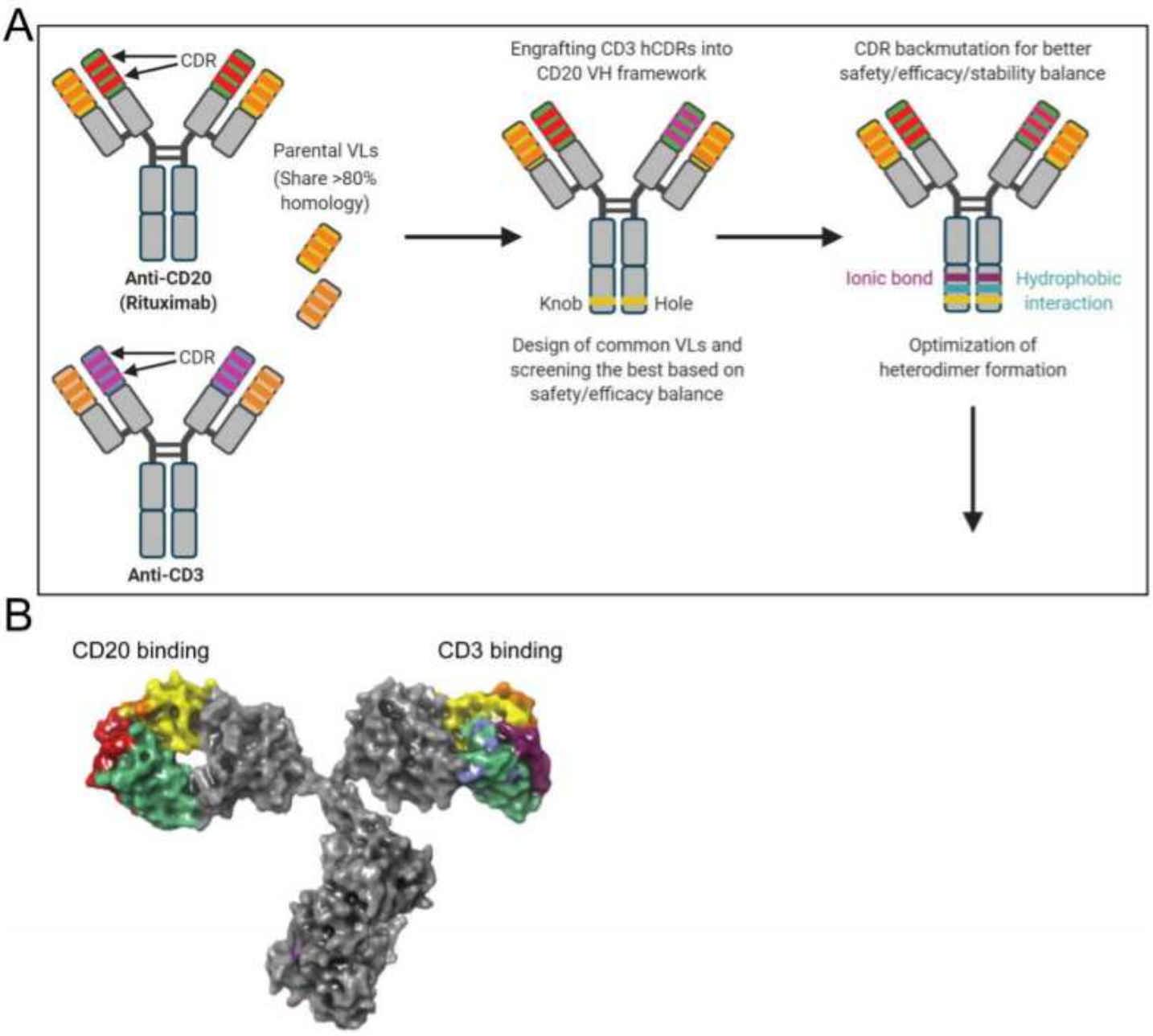

Figure 1

Computer aided design process of the “imbalanced” BsAb GB261. HCDRs in one arm of the parental CD20 (Rituximab) was replaced by the HCDRs of parental CD3 antibody to construct the preliminary CD20/CD3 BsAb. Several common VL sequences that share homology to VL (CD20) and VL (CD3), and may lead to loss of binding to CD3 but maintains binding to CD20 were designed and paired with the two VHs. These IgG like BsAbs with different common VL candidates were constructed in the “knob into hole (KIH)” format. Then, T cell activation assays were performed to select the lead BsAb molecule with the best safety/efficacy balance. Then, new mutations in the Fc domain were introduced to further improve heterodimer formation. In addition, the pI of the two BsAb VHs were differentiated by introducing new

mutations in the VH non-CDR framework regions. The deimmunization mutations were also introduced. The final lead molecule GB261 v4b was selected based on great safety/efficacy balance as well as great manufacturability represented by high expression level, high heterodimer formation percentage, easy purification process, and great biochemical and biophysical characterization data.

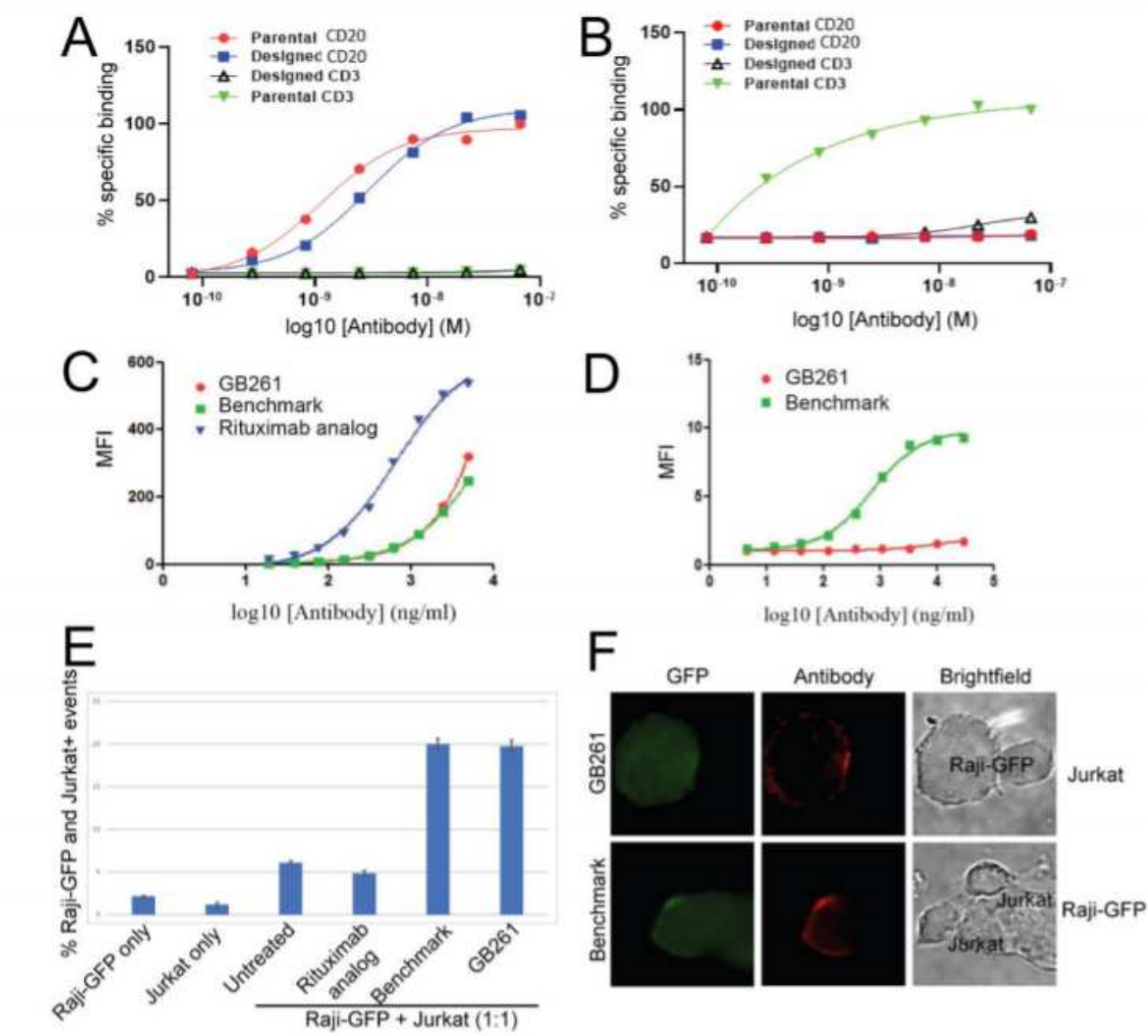

Figure 2

GB261 is much weaker than BM in CD3 binding but is comparable in CD20 binding. A) Binding of designed CD20 and CD3 antibodies to CD20+ Raji cells, compared with those of the parental CD20 and CD3 antibodies. Cells were incubated with antibodies, labeled with Cy3-conjugated Goat anti-human antibody, followed by FACS. The binding was presented as the percentage of cells positive for staining. B) Antibodies tested in Fig. 2A were examined for binding to CD3+ Jurkat cells using the same method. C)

Binding of GB261, BM and Rituximab analog to Raji cells. The cells were labeled with a Cy3-conjugated Goat anti-human antibody and analyzed using FACS. The binding was quantified as the mean fluorescent intensity (MFI) of staining. D) Binding of GB261 and BM to Jurkat cells. E) Raji-GFP cells were mixed with Jurkat cells pre-stained with CellVue Claret Far Red fluorescent dye at 1:1 ratio and incubated overnight with 20 µg/ml antibodies, followed by the detection of cells by FACS. The events double positive for GFP and fluorescent dye were counted as bridged Raji-GFP and Jurkat cells. F) Raji-GFP cells were mixed with unstained Jurkat cells at 1:1 ratio, incubated with 20 µg/ml antibodies, and stained with DyLight 594-conjugated goat anti-human IgG. Two representative images showing the bridging of Raji-GFP cells and Jurkat cells in the presence of antibodies are shown. The display of the images has been adjusted non-uniformly for representation.

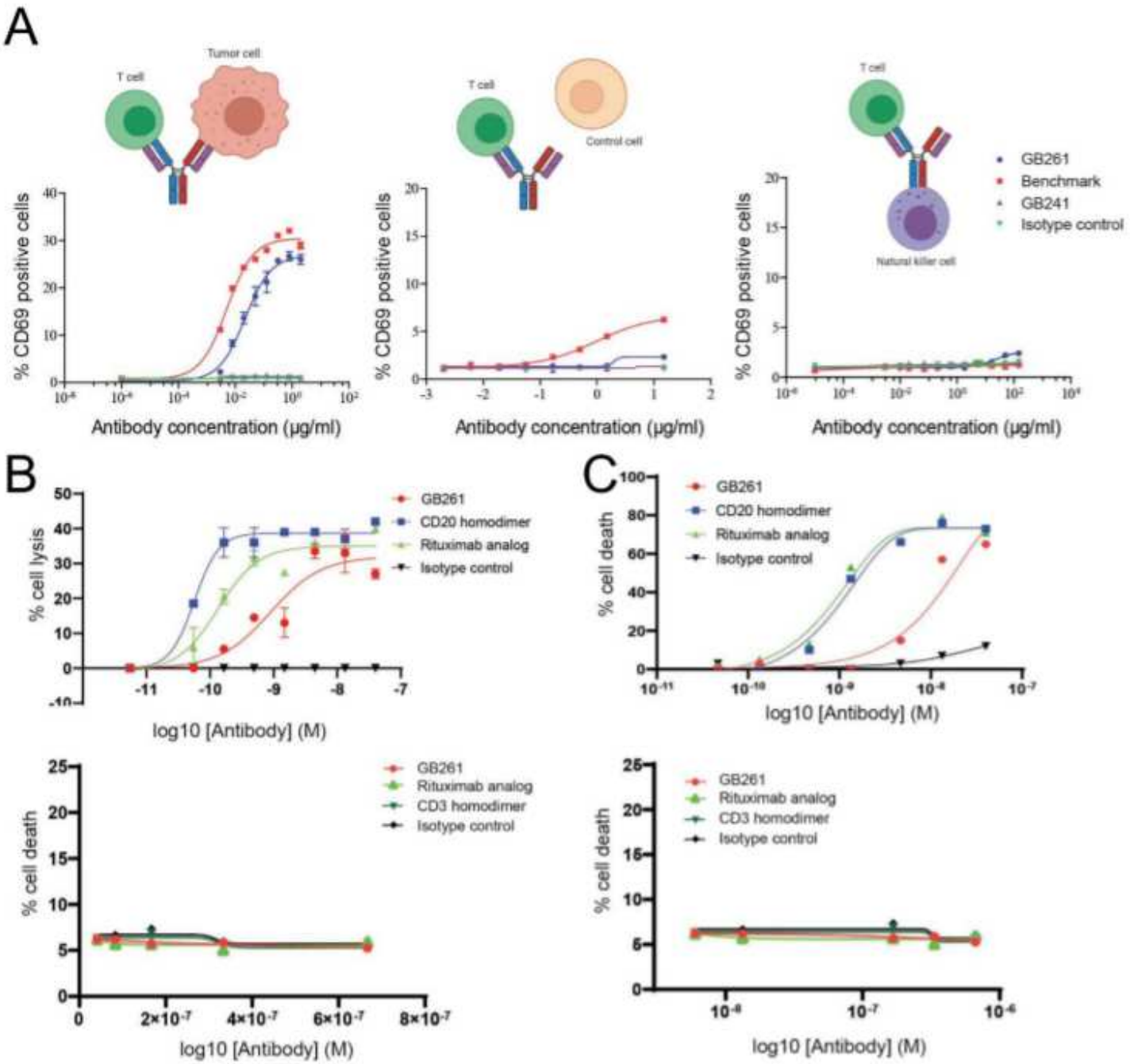

Figure 3

GB261 has balanced safety/efficacy. A) Jurkat (T cell) activation by GB261, BM, GB241, and an isotype IgG as performed by co-incubating with Raji (left), CHO cells (middle) and NK92-CD16 cells (right) at 1:1 ratio. The cells were labeled with anti-CD69 antibodies conjugated to PE and analyzed by flow cytometry. B) Upper panel, ADCC induced by either GB261, an anti-CD20 homodimer, Rituximab analog, or an isotype IgG. Raji cells labeled with Calcein AM were treated with antibodies and incubated with NK-92-CD16 cells. Lower panel examines whether the GB261-induced ADCC kills T cells that it binds to. Human PBMC were incubated with GB261, Rituximab analog, a CD3 mAb, and the isotype control antibody. T cell viability was analyzed by FACS. C) Upper panel, CDC induced by either GB261, a CD20 homodimer, Rituximab analog, or an isotype IgG. Raji cells labeled with Calcein AM were treated with antibodies and incubated with complement-enriched human serum. Lower panel, Jurkat cells were incubated with antibodies as described in C Upper panel and the viability of the cells were analyzed by FACS.

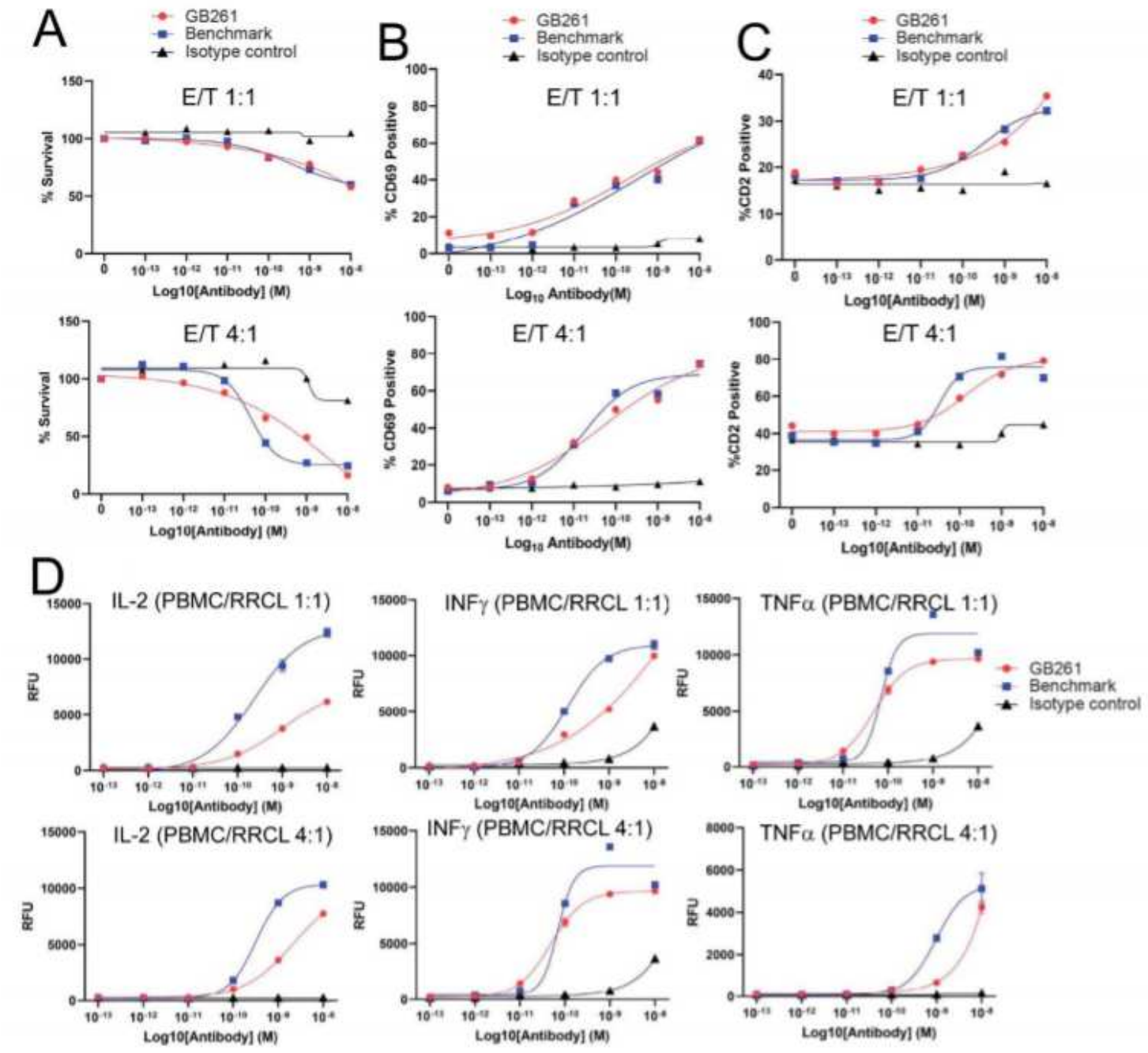

Figure 4

GB261 and BM has similar effects on tumor cell killing, T cell activation and total T cell number, but GB261 induces less cytokine release compared to BM. hPBMC were mixed with RRCL-GFP-Luc cells at E:T 1:1 or 4:1 ratios and incubated with test antibodies GB261 and BM, or an isotype control antibody for 48 hours. The cells were labeled with CD2-APC and CD69-PE antibodies followed by analyzing with FACS. A) RRCL-GFP-Luc killing was assessed by the percentage of survived GFP positive cells. B) T cell activation was determined by the percentage of CD2+/CD69+ cells, and C) total T cell number was assessed by the percentage of CD2+ cells. D) The experiment was performed as described above, and the release of cytokines was detected by ELISA using the cell culture supernatants.

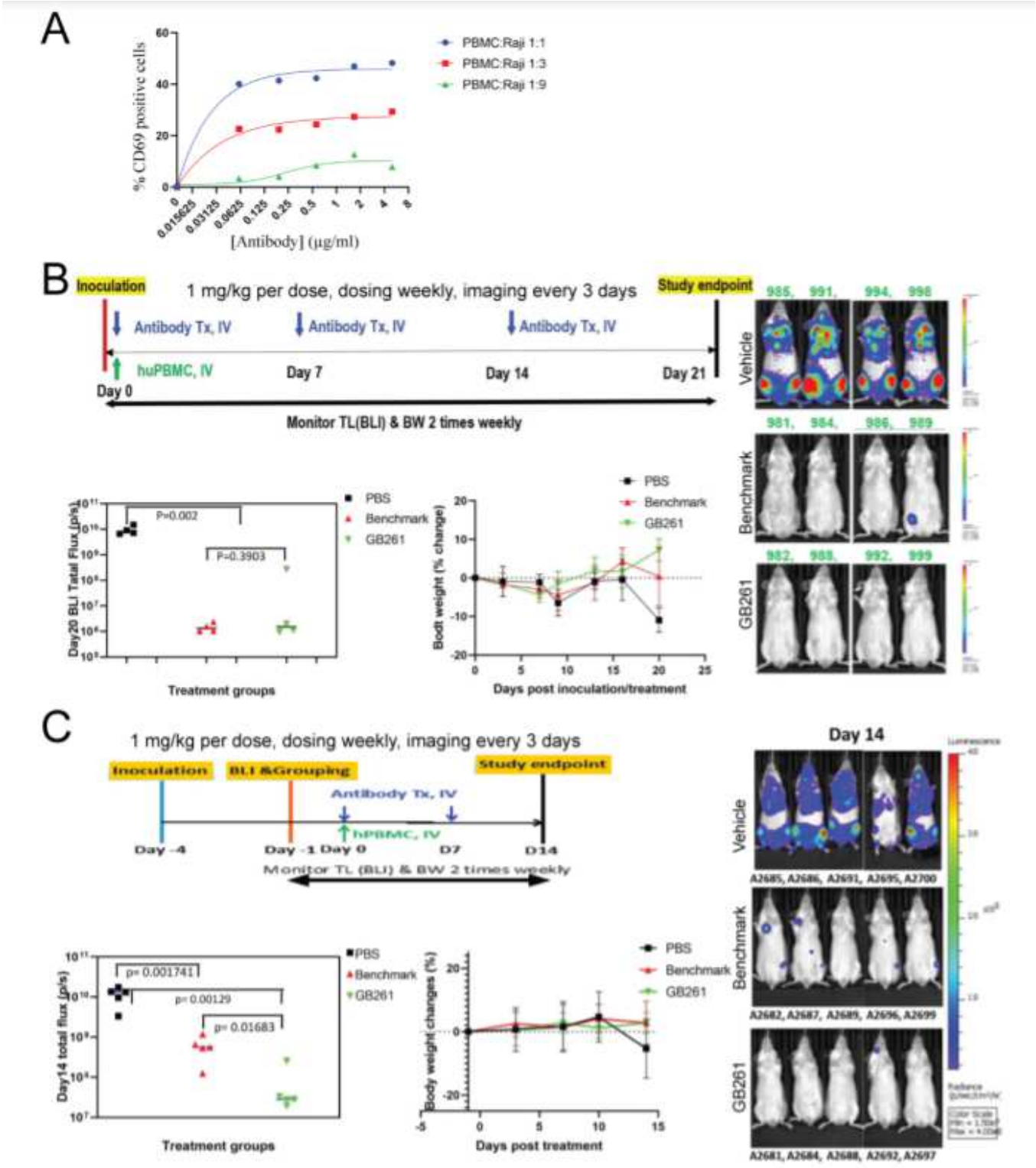

Figure 5

GB261 has better efficacy compared to the BM at low T/B cell ratios. A) hPBMC and Raji-GFP-Luc cells were mixed at ratios of 1:1, 1:3 and 1:9 and incubated with indicated concentrations of GB261 or an isotype IgG. T cell activation was assessed by measuring CD69+/CD2+ T cells by FACS. The background T cell activation by the isotype control antibody was subtracted from the values obtained for GB261. B) RRCL-GFP-Luc cells were mixed with HLA matching (HLA-DR3+) hPBMC at 1:1 ratio. Then, the cells were

mixed with PBS, GB261, or BM, and subsequently injected into mice by i.v. (4 mice/group). Each mouse received 5 x 105 RRCL-GFP-Luc cells and 5 x 105 PBMC, with or without the antibodies. An amount of 20 μg of antibodies were administered at day 0 and day 7, and 60 μg of antibodies were administered at day 14. The mice were monitored for a total period of 21 days and the tumor luminescence was imaged every 3 days. The workflow, total tumor luminescence on Day 20, and the percentage body weight change of the mice from the initial weight are shown in the upper, lower left, and lower right panels, respectively. C) The mice were first inoculated by RRCL-GFP-Luc cells. After 4 days, the HLA matching hPBMC were mixed with PBS (Control) or 1 mg/kg test antibodies GB261 or BM, and injected into mice by i.v (5 mice/group). At this point, the T:B cell ratio is about 1:8. Each mouse received 5 x 105 RRCL-GFP-Luc cells and 5 x 105 PBMC. The antibodies were administered at day 0 and day 7 and the mice were monitored for a total period of 14 days. The tumor luminescence was imaged every 3 days. The workflow, total tumor luminescence on Day 14, and the percentage body weight change of the mice from the initial weight are shown in the upper, lower left, and lower right panels, respectively.

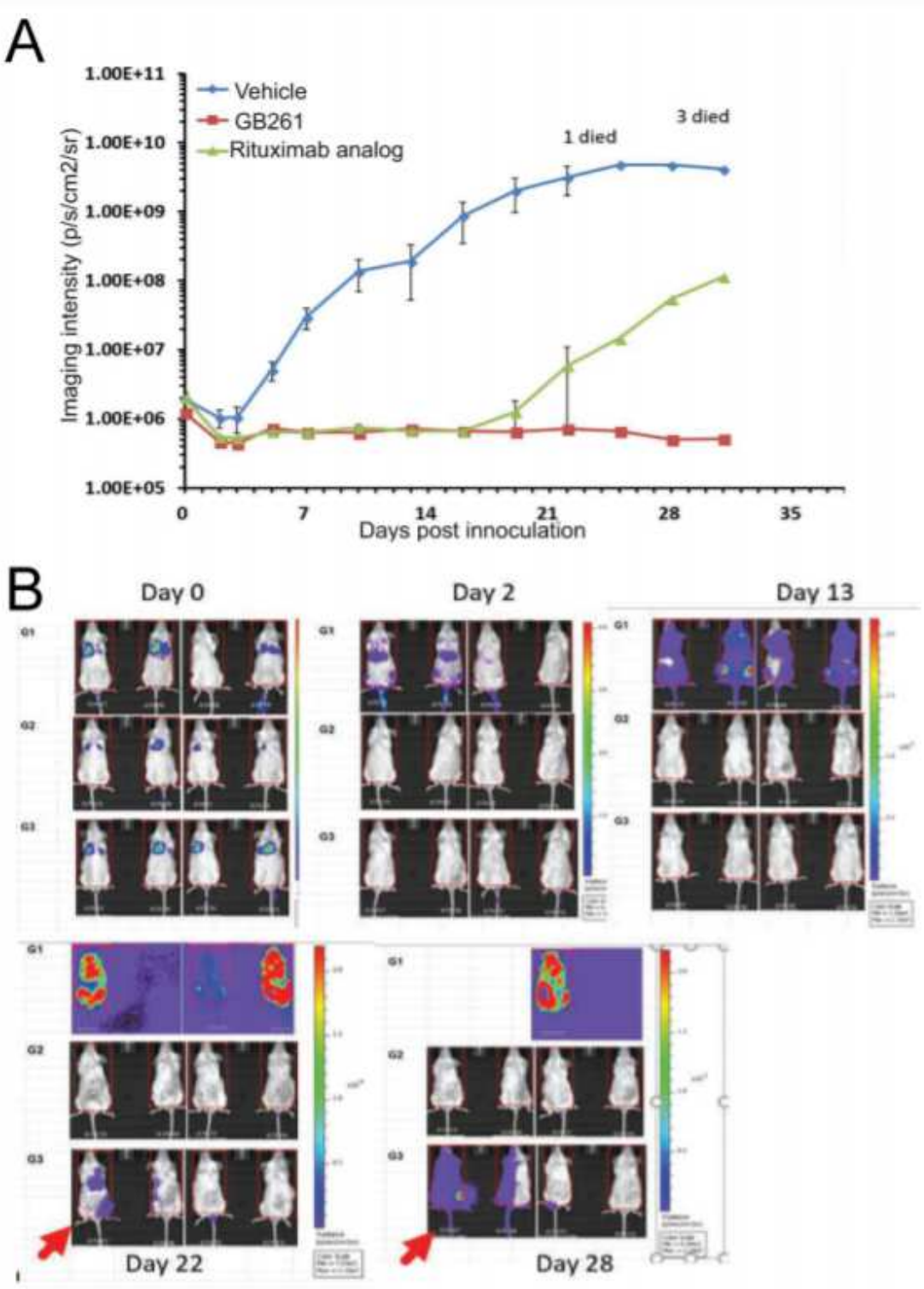

Figure 6

. GB261 prevents tumor relapse in an in-vivo mouse model. Raji-GFP-Luc cells and hPBMC were mixed with either PBS, GB261, or Rituximab, and injected into mice by i.v. A total of 4 animals were used per each treatment group. The mice received 5 x 10 5 Raji-GFP-Luc cells, 2.5 x 106 PBMC, and 60 µg of each antibody. They were imaged for the tumor luminescence at 15 minutes post-i.v., and then at day 2, day 3

and every 3 days after that. The mice were monitored for a total period of 31 days. The tumor volume was quantified (A) and the luminescent images of the mice are shown (B).

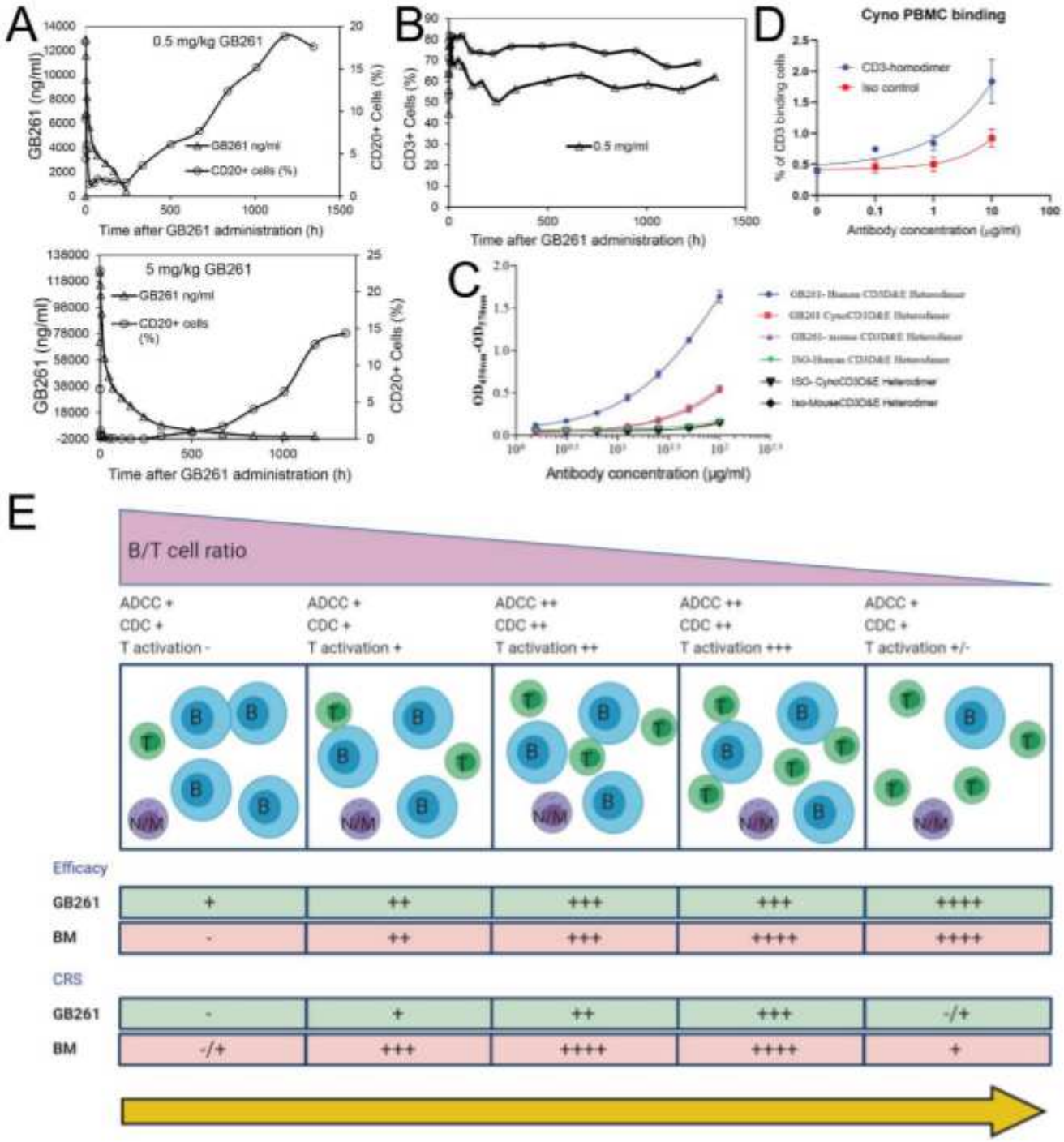

Figure 7

Effects of GB261 on CD20+ and CD3+ lymphocytes in Cynomolgus monkeys. A) CD20+ lymphocytes and GB261 levels in Cynomolgus monkey blood after administration of 0.5 mg/ml or 5 mg/ml of GB261. Lymphocytes are mean of 2 Cynomolgus monkeys. GB261 levels are mean of 9 Cynomolgus monkeys. B) CD3+ lymphocytes of Cynomolgus monkeys after administration of 0.5 mg/ml or 5 mg/ml of GB261. Data are mean of 2 Cynomolgus monkeys. C) The binding of GB261 or an isotype control antibody at

indicated concentrations to recombinant human, Cynomolgus, and mouse CD3D and E heterodimers were assessed by ELISA. The binding was measured as the optical density (OD) values at 450 nm and 570 nm. D) Binding of CD3 homodimer and an isotype control antibody to Cynomolgus PBMC, determined by FACS. E) A model depicting the mechanisms of action of GB261, compared with those of BM.

Supplementary Files

This is a list of supplementary files associated with this preprint. Click to download.

- SupplementarymaterialsbyCaietal030521.pdf